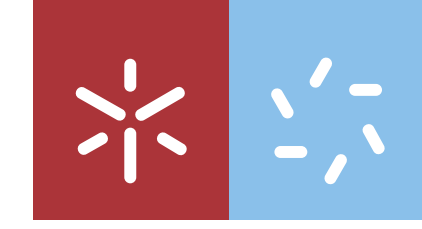Universidade do Minho
Escola de Ciências

Rute Lúcia Loureiro Rego

Isolation and characterization of phages targeting the phytopathogenic bacteria of *Actinidia*

Dezembro 2021

Isolation and characterization of phages targeting the phytopathogenic bacteria of *Actinidia*

Rute Rego

UMinho | 2021

Universidade do Minho
Escola de Ciências

Rute Lúcia Loureiro Rego

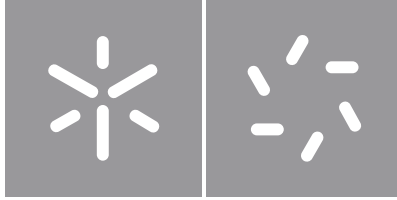# Isolation and characterization of phages targeting the phytopathogenic bacteria of *Actinidia*

Master Thesis
Plant Molecular Biology, Biotechnology and
Bioentrepreneurship

Work performed under the guidance of
Doctor Francisca Rodrigues Reis
Doctor Diana Priscila Penso Pires

Dezembro de 2021

DIREITOS DE AUTOR E CONDIÇÕES DE UTILIZAÇÃO DO TRABALHO POR TERCEIROS

Este é um trabalho académico que pode ser utilizado por terceiros desde que respeitadas as regras e boas práticas internacionalmente aceites, no que concerne aos direitos de autor e direitos conexos. Assim, o presente trabalho pode ser utilizado nos termos previstos na licença abaixo indicada. Caso o utilizador necessite de permissão para poder fazer um uso do trabalho em condições não previstas no licenciamento indicado, deverá contactar o autor, através do RepositóriUM da Universidade do Minho.

Acknowledgments

STATEMENT OF INTEGRITY

I hereby declare having conducted this academic work with integrity. I confirm that I have not used plagiarism or any form of undue use of information or falsification of results along the process leading to its elaboration.

I further declare that I have fully acknowledged the Code of Ethical Conduct of the University of Minho.

University of Minho, 29 of December 2021

_____

Rute Lúcia Loureiro Rego

Abstract

Isolation and characterization of phages targerting the phytopathogenic bacteria of *Actinidia*

Pseudomonas syringae pv. *actinidiae* (Psa) is the causal agent of bacterial canker in kiwifruit (*Actinidia deliciosa*), leading to severe symptoms in plants and consequent considerable production and financial losses. Current methods for controlling this disease rely on the use of copper-based products and, in countries outside the European Union, in the use of antibiotics. These products, besides being considered phytotoxic, can lead to the spread of resistance to both copper and antibiotics. With the increasing need to obtain safe and effective biocontrol strategies against this pathogen, this study focused on the isolation and characterization of (bacterio)phages for the control of Psa. A collection of Psa strains was characterized by PCR and phenotypical analysis, such as Biolog GEN III and phages were isolated from branches, buds, leaves, petals, sepals, and stamens from kiwifruit plants in orchards in the North of Portugal. Phages were isolated using the enrichment procedure with Psa strains CFBP 7286 and P84 as possible hosts, and the lytic spectra of 6 selected phages were tested against the Psa collection. Two phages displayed broader host ranges (between 71% and 84% of efficacy among Psa strains) were selected for further analysis. Phage stability was studied at different temperatures (-20° to 60°C), pH (1-13) and UV light, and it was observed that the two phages were stable between -20°C and 50°C, pH range of 3 to 11 and UV light at 366 nm up to 180 min. The morphological characterization of phages was done by Transmission Electron Microscopy and genome sequencing. *In vitro* efficacy assays showed that phage 177T was able to reduce the number of CFUs after 4h of inoculation and keeping the bacterial load at low levels for up to 24h post-infection with MOI=1. Phage VC3 was able to decrease the OD_{600} through 24h. In a preliminary test, the infection of Psa and phage in kiwi plants was examined, and the evolution of symptoms after 12 days of inoculation with just Psa was observed. One phage has been sequenced and confirmed to be lysogenic, prophages might be employed to combat illnesses caused by harmful bacteria. In this study was possible to highlight the potential of phages as promising biocontrol agents against Psa, that could be used in the future to replace copper compounds and antibiotics.

Keywords: *Actinidia deliciosa*; bacterial canker; bacteriophages; kiwifruit; *Pseudomonas syringae* pv. *actinidia* (Psa)

Resumo

Isolamento e caracterização de fagos contra bactérias fitopatogénicas na *Actinidia*

Pseudomonas syringae pv. *actinidiae* (Psa) é o agente da doença do cancro bacteriano da Actinidea (*Actinidia deliciosa*), e é responsável por perdas consideráveis produtivas e financeiras, fazendo com que as plantas sofram sintomas severos. Os métodos atuais de controlo da doença contam com o uso de produtos à base de cobre e, em países fora da União Europeia, com o uso de antibióticos. Esses produtos, além de serem considerados fitotóxicos, podem levar ao aparecimento da resistência tanto ao cobre quanto aos antibióticos. Com a necessidade cada vez maior de se obterem estratégias biológicas, seguras e eficazes contra esse patogénio, este estudo abordou o isolamento e a caracterização de bacteriófagos para o controlo de Psa. Uma colecção de estirpes de Psa foi caracterizada por métodos moleculares e análises fenotípicas, como Biolog GEN III. Os fagos foram isolados de ramos, botões, folhas, pétalas, sépalas e estames de plantas de kiwi em pomares no Norte de Portugal usando o procedimento de enriquecimento com as estirpes Psa CFBP 7286 e P84 como possíveis hospedeiros, e o espectro lítico de 6 fagos selecionados foram testados contra a coleção de Psa. Dois fagos exibiram eficácia entre estirpes de maneira mais ampla (entre 71% e 84% de eficácia entre as estirpes de Psa) e foram selecionados para determinar análises posteriores. A estabilidade dos fagos foi estudada em diferentes temperaturas (-20° a 60°C), pH (1-13) e luz UV, e foi observado que os dois fagos eram estáveis entre -20°C e 50°C, de pH de 3 a 11 e luz UV a 366 nm até 180 min. A caracterização morfológica foi feita por Microscopia Eletrônica de Transmissão e procedeu-se à sequenciação do genoma. Ensaios de eficácia *in vitro* mostraram que o fago 177T foi capaz de reduzir o número de UFC após 4h de inoculação e manter a carga bacteriana em níveis baixos por até 24h pós-infecção com MOI = 1. O fago VC3 foi capaz de diminuir a OD_{600} ao longo de 24h. Num teste preliminar, foi examinada a infeção de Psa e fago em plantas de kiwi, e foi observada a evolução dos sintomas após 12 dias de inoculação apenas com Psa. Neste estudo apenas um fago foi sequenciado e confirmado como lisogénico, os profagos podem ser benéficos para combater doenças prejudiciais causadas por bactérias patogénicas. Neste estudo foi possível destacar o potencial dos fagos como agentes de biocontrolo promissores contra Psa, que podem ser usados no futuro para substituir compostos de cobre e antibióticos

Palavras-chave: *Actinidia deliciosa*; cancro bacteriano; bacteriófagos; kiwi; *Pseudomonas syringae* pv. *actinidia* (Psa)

Index

List of abbreviations

AMPs – Antimicrobial Peptides

ASM – Acibenzolar-S-methyl

CFU – Colony forming unit

DF – Dilution Factor

DNA - Deoxyribonucleic Acid

EDTA - Ethylenediamine tetraacetic acid

KOH – Potassium hydroxide

MOI – Multiplicity of Infection

OSGC – One-Step Growth Curve

OD – Optical Density

PCR – Polymerase Chain Reaction

PFU – Plaque forming unit

Psa – *Pseudomonas syringae* pv. *Actinidiae*

RNA – Ribonucleic Acid

SDS - Sodium Dodecyl Sulfate

TAE - Tris-Acetate-EDTA

TEM - Transmission Electron Microscopy

TSA – Tryptic Soy Agar

TSB – Tryptic Soy Broth

List of figures

List of tables

1. Introduction

1.1. *Actinidia* cultivation and kiwifruit production

The genus *Actinidia,* belongs to the *Actinidiacea* family, it has 76 species described, and 125 taxa worldwide (Zehra *et al.*, 2020). The most popular species are *Actinidia deliciosa* (green kiwifruit) and *Actinidia chinensis* (yellow kiwifruit) (Guroo *et al.*, 2017). Although *A. chinensis* has a sweeter and aromatic fruit, its shelf life is very reduced, limiting its commercialization. Unlike *A. deliciosa* and its predominant cultivar, *A. deliciosa* "Hayward" has a bigger fruit and is more suitable for production, having longer shelf life (Drzewiecki *et al.*, 2016; Guroo *et al.*, 2017). Besides *A. deliciosa* and *A. chinensis,* other species are included in this genus: *A. Melanandra* (red kiwifruit), *A. arguta* (baby kiwifruit), *A. purpurea* (purple kiwifruit), *A. kolomikta* (artic kiwifruit), *A. polygama* (silver vine) and *A. eriantha* (velvet vine) (Guroo *et al.*, 2017).

Actinidia species was first described in 1750 as ornamental plants found in China. Although seeds of *A. chinensis* were sent to Europe, it was only in 1904 when *A. deliciosa* was inserted in New Zealand that the great exploitation of the potential of the kiwifruit started *(Zhen et al.*, 2004; Zehra *et al.*, 2020).

Kiwifruit industry has a strong economic impact with an annual production reaching 4.3 million tons worldwide in 2019 (IndexBox, 2020). The biggest Kiwifruit producers are China, Italy and New Zealand, and this massive production leads to a retail market value of ten billion euros(Donati *et al.*, 2020). Only in New Zealand the production of kiwi led to an annual revenue of one billion $NZ (Cameron and Sarojini, 2014).

In Portugal, Actinidia was introduced later, in 1973, but it was after 1980 that the interest in kiwi production increased, due to its good productivity at that time (Franco, 2008). Kiwi production can reach 32 thousand tons and, in 2019 alone, there was a 126% increase in the installation of kiwi orchards (INE, 2020). Over time, the installation of Actinidia orchards has spread throughout the country, but its largest production is found in the regions Entre Douro e Minho and Beira Litoral (Moura *et al.*, 2015).

Although there is a large production of kiwi, this cultivation, like many others, suffers very serious diseases caused by phytopathogenic bacteria. One of the most serious problems is the bacterial canker of kiwifruit caused by *Pseudomonas syringae* pv. *actinidiae*, which is considered

the most significant limiting factor in kiwifruit production that leads to tremendous economic losses (Morán, 2018).

1.2. Overview of *Pseudomonas syringae* pv. *actinidiae*

1.2.1. Morphology and Taxonomy

Pseudomonas syringae pv. *actinidiae* (PSA) is an gram-negative bacteria with a white circular and convex colony (Figure 1) (Takikawa *et al.*, 1989). Since PSA is considered the biggest threat to the production of kiwi worldwide, it has been included on the A2 list of European Plant Protection Organization as a quarantine strain(Abelleira *et al.*, 2014; EPPO 2021).

Figure 1.1- Colonies of *Pseudomonas syringae* pv. *actinidiae* in King's B medium.

Psa is divided by 6 different populations (also known as biovars) that are capable to infect Actinidia with distinct levels of virulence, which are denominated by Psa biovar 1, 2, 3, 4 ,5 and 6.

Psa biovar 1 was the first strain to be described in Japan in 1984 causing massive economic losses in the kiwifruit industry. Later, in 1992, it was also detected in Italy causing less damage when compared to the outbreak in Japan due to climatic factors. These strains have in their genome phaseolotoxin, which is a toxin responsible for the halo symptoms on the leaves.

Psa biovar 2 was only found in South Korea, causing major economic losses after infection of *A. deliciosa* and *A. chinensis*. This one doesn't produce phaseolotoxin but instead has coronatine in the genome (Cameron and Sarojini, 2014; Figueira *et al.*, 2020). Coronatine is known to be a

toxin that enhances bacterial growth and develop the disease symptoms, which can be produced by several *Pseudomonas syringae* strains (Zheng *et al.*, 2012).

Psa biovar 3 is the most aggressive population of them all and, unlike Psa Biovar 1 and 2, this one does not present phaseolotoxin or coronatine (Wicaksono *et al.*, 2018). It can be very destructive and cause severe economic losses and is responsible for the outbreaks in Italy, France, Spain, Portugal, New Zealand, Chile, China, Korea and Japan. Psa3 is also responsible for the bacterial canker in Actinidia (Abelleira *et al.*, 2014; He *et al.*, 2019; Vaz *et al.*, 2018).

Psa biovar 4 was found in New Zealand and Australia (Cameron and Sarojini, 2014); this population was unable to cause infections and is considered low virulent, causing only leaf spots and no damage to kiwifruit, after comparing different characteristics on phylogenetic and phenotypic analysis it was decided to rename this population to *Pseudomonas syringae* pv. *actinidifoliorum* (Psaf) (Abelleira *et al.*, 2015; Cunty *et al.*, 2014; Morán, 2018).

Psa biovar 5 and biovar6 were both found in Japan in limited areas (Morán *et al.*, 2018). It was verified that biovar 5 is more related to biovar 2 than the other populations of Psa, but biovar 5 does not produce both coronatine and phaseolotoxin(Figueira *et al.*, 2020; Fujikawa & Sawada, 2016) Biovar 6 produces both toxins and is more related to biovar 1 and 3(Sawada *et al.*, 2016).

1.2.2. Propagation and Symptoms

Psa is common in the surface of plants, mostly in leaves, buds, twigs and flowers (Figueira *et al.*, 2020). Psa infection occurs with temperatures ranging between 12°C and 18°C, being the autumn and spring seasons two moments of high risk for plant infection and bacterial dissemination (Vanneste *et al.*, 2011).

There are several sources of plant infection by Psa, as this population also resides outside Actinidia without causing any symptoms. The sources of infection of Psa can be over short distances, when infected plants interact in an orchard of healthy plants. Also, the use of pruning material or other material used on infected plants is also a source of infection and helps spreading the bacteria. Climatic conditions such as rain, frost and wind can also contribute to the spread of the bacteria among plants: rain and frost help Psa to enter tissues and the wind can take infected pollen to healthy plants within a short distance (Vanneste, 2013; Vanneste *et al.*, 2011) The disease symptoms also can appear during the spring, on leaves, flowers and branches (Figure 1.2) (Abelleira *et al.*, 2015). Although with less favorable temperatures, in winter, with frost, Psa

symptoms can be observed. As the disease aggravates it mixes with the dark coloured bark tissue producing a red rusty exudate (Vanneste *et al.*, 2011).
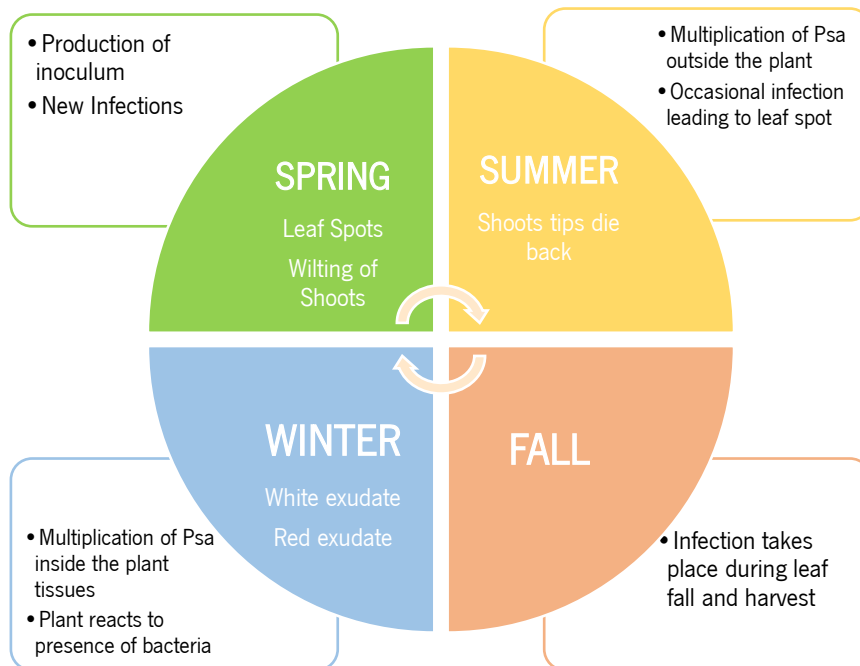
Figure 1.2- Life cycle of *Pseudomonas syringae* pv. *actinidiae*. In each season it is described the major symptoms (inside the circle), and the justification of why these symptoms occur (outside the circle). Adapted from Vanneste *et al.*, (2011).

The symptoms of Psa are identified by brown necrotic spots on the leaves, surrounded, or not, by a yellow halo, necrosis and abortion of flower buds and red or white exudates in the trunks and branches (Figure 1.3) (Butler *et al.*, 2013; Vanneste, 2013). When the bacteria begin to proliferate throughout the plant, the symptoms are severe: wilt on the branches, leaf fall and dehydration of the fruits, which end up losing their commercial value, and finally, Psa can lead to the death of the plant or death of the entire orchard (Carvalho *et al.*, 2017).

To infect the internal tissues of the plant, Psa needs to go through the epiphytic phase to the endophytic phase. The bacteria enter naturally through the opening of the stomata or also through lesions in the trichomes, leaf abscission and fresh cuts. In the winter, with the lesions caused by frost, the entry of the bacteria into the plant is facilitated and later on can cause its multiplication (Figueira *et al.*, 2020; Spinelli *et al.*, 2011).Trichomes on kiwi are able to create a favorable environment for the growth of bacteria due to their retention of humidity and to its hairy

structures, also protecting the bacteria from adverse conditions (Figueira *et al.*, 2020; Spinelli *et al.*, 2011).

Once in the endophytic phase, the bacteria can migrate between the leaves, shoots and twigs through the apoplast and then through xylemic vessels (Donati *et al.*, 2020; Figueira *et al.*, 2020). Psa can invade the majority of the tissues of the plant and can create an systemic infection when the bacteria migrates to the xylem (Spinelli *et al.*, 2011).
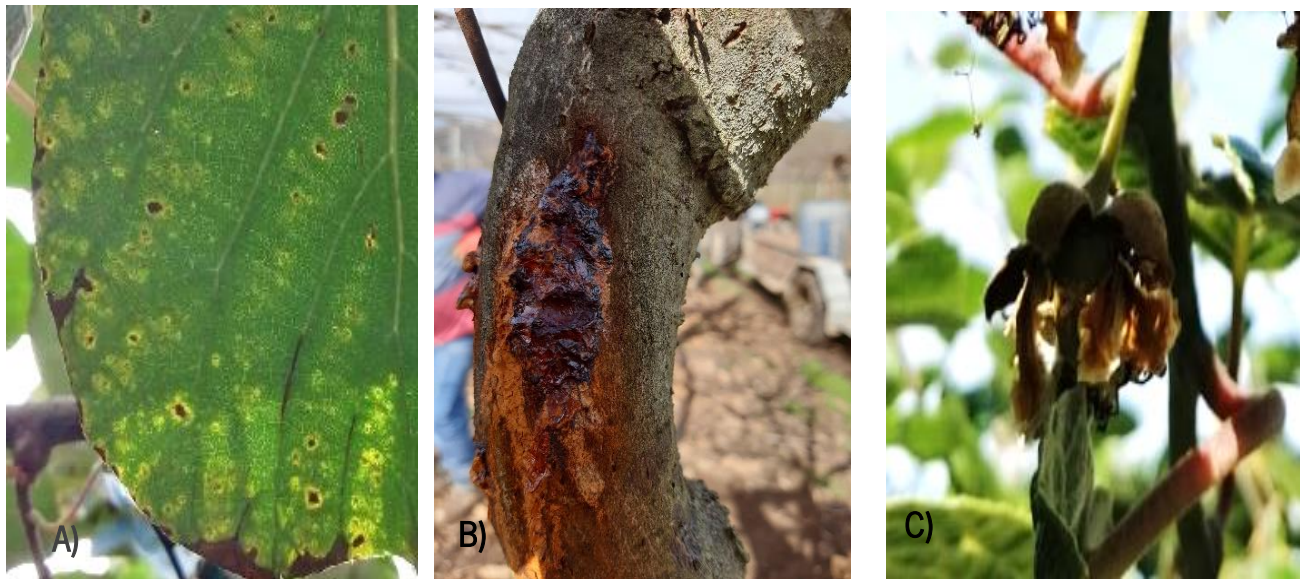
Figure 1.3- Symptoms of *Pseudomonas syringae* pv. *actinidiae*. A) Brown spots surrounded by a yellow halo; B) Red exudate on infected trunk; C) Abortion of flower buds. (Kiwi GreenSun, SA, 2020).

1.2.3. Current methods for Psa control

Currently, there is no product or solution that eliminates Psa completely, but there are different means of combat that aim to control the effects of the bacteria on the plants (Carvalho *et al.*, 2017).

To arrest the spread of Psa among plants in an orchard, the implementation of good plant cultivation practices is essential such as the disinfection of cut material used in infected plants and the elimination and destruction of the infected organs (DGAV, 2013). In countries of the European Union, it is mandatory that all the transited plants have a phytosanitary passport to prevent the

entry and spread of Psa (Commission Implementing Decision No. 2012/756 / EU, of 5 December) (Borg, 2012).

Copper-based chemicals (copper hydroxide and copper sulfate) are commonly used products to fight bacterial canker in kiwifruits; however, these treatments should be avoided due to its phytotoxicity, due to the decrease of soil diversity, and also due to the risk of spreading resistance of Psa to these compounds. In Asian countries and in New Zealand, antibiotic products (like streptomycin) are also used to fight this bacterial disease; however, according with the 2004/129/CE Decision of the European Commission on the 91/414/CEE Directive, the use of antibiotics as phytopharmaceuticals are not allowed in the European Union (Bryne, 2003; Bukman, 1991; Cameron & Sarojini, 2014; Carvalho *et al.*, 2017; Mariz-Ponte *et al.*, 2021). Both of the chemical options mentioned above have shown phytotoxicity problems, and can cause resistance in bacteria and leave residues on fruits (Donati *et al.*, 2014). In addition, streptomycin can lead to chlorosis and "cupping" on leaves, while copper can damage stalks and leaves (Cameron and Sarojini, 2014).

Besides copper and streptomycin, others compounds were studied to realize the ability to control Psa,over the last years several alternatives of biological control have been studied as substitutes for chemical products. One of these studies was with terpenes, two monoterpenes, geraniol and citronellol were able to create an inhibitory effect on *in vitro* assays against Psa. These monoterpenes disturb the lipid membrane, changing its permeability leading to cell death (Cameron & Sarojini, 2014; Ferrante & Scortichini, 2010). Chitosan, that is obtained from shrimp shells was also tested against Psa and has the advantage of being both biocompatible and biodegradable (Donati *et al.*, 2014). Chitosan interacts with the negative charged membranes of the pathogen that leads to the leakage of the intracellular content and it can also inhibit the microbial growth (Cameron & Sarojini, 2014). Even though chitosan can decrease the epiphytic inoculum loads, once the pathogen enters the plant tissue, it is no longer effective (Donati *et al.*, 2014).*Bacillus subtilis* is one of the most used biologic alternative, *Bacillus subtilis* has the advantage to create antibiosis by competing with the pathogenic bacteria by killing it or by reducing its growth and, can also induce systemic resistance. It is used in Gray Mold, provoked by *Botrytis cinerea*, Bacterial spot (*Xanthomonas* spp.), *Pseudomonas syringae* pv. *tomato* , among others bacterial or fungal strains(Carvalho *et al.*, 2017; Stewart *et al.*, 2011). Essential oils like clove bud (*Syzigium aromaaticum*), thyme (*Thymus vulgaris*) and oregano (*Origanum vulgare*) were also tested for their antimicrobial activity and production of radical reactions when interacting with lipids

of the cell membrane, causing cell death (Pucci *et al.*, 2018; Song *et al.*, 2016; Vavala *et al.*, 2016). Recently, antimicrobial peptides (AMPs) began to be studied for its protective power of the host in attacks against the pathogen and for its low toxicity (Mariz-Ponte *et al.*, 2021). AMPs are constituted with less than 50 amino acids, are amphipathic and have a cationic charge that become a great binding site with the plasmatic membrane of Psa that has anionic groups. This creates a displacement of the metal ions, damaging the outer membrane and creating access to the inter membrane. This process allows the leakage of intercellular material and can provoke disintegration of the membrane and lysis (Cameron & Sarojini, 2014). The study of plant-induced resistance was also deepened, Acibenzolar-S-methyl (ASM) was authorized as a biological product due to the emergency to control the bacterial canker caused by Psa in Italy (Bion® or Actigard®)(Pucci *et al.*, 2018). ASM belongs to the benzothiadiazole chemical group and operates as a functional analogue of salicylic acid leading to an increase at the resistance to pathogens and an upregulation of pathogenesis-related genes (Cameron & Sarojini, 2014; Jong *et al.*, 2019). Nevertheless, resistant inducers can be effective in controlled conditions but the host response in the field could be variable and also lead to a decrease of fruit quality and production(Reglinski *et al.*, 2013). Lastly, a great interest in the study of bacteriophages has arisen as a biological control against Psa, bacteriophages are viruses that have the advantage of being able to control bacterial infections, without affecting the normal microbiota (Pinheiro *et al.*, 2020) and also has a high specificity of the host with strong lytic activity (Ni *et al.*, 2020).

1.3. Biocontrol of phytopathogenic bacteria on *Actinidia* using bacteriophages

1.3.1.   Bacteriophages - definition, classification and life cycles

Bacteriophages (also known as phages) are viruses that specifically infect, and in many cases, kill bacteria without affecting the host's microbiota (Chan *et al.*, 2013; Frampton *et al.*, 2012). They were described in 1915 and also in 1917 by Twort and d'Hérelle, respectively, and soon after started being used as therapeutic agents against bacterial diseases (Terms, 2011; Twort, 1915). Although the early promising results and effective treatments, the use of phages has drastically decreased with the introduction of antibiotics. However, the extensive use of antibiotics over time led to the spread of bacterial resistance throughout the world and so, these compounds became increasingly ineffective. This fact has triggered the interest on phages that reemerged as

a promising and attractive alternative to antibiotics and other chemicals to combat bacterial pathogens (Sieiro *et al.*, 2020).

As phages are considered the most abundant entities on Earth, they can be found in many different environments were their bacterial hosts are present (Clokie *et al.*, 2011). Most of the phages belong to the *Caudovirales* order, which is characterized by grouping tailed phages. Recently it was added new families to this order but the three largest families are *Myoviridae* that represents phages with contractile tails, *Siphoviridae,* representing phages with long, noncontractile tails and *Podoviridae* that englobes phages with short, noncontractile tails (Maniloff & Ackermann, 1998; Turner *et al.*, 2021; Yu *et al.*, 2016) .
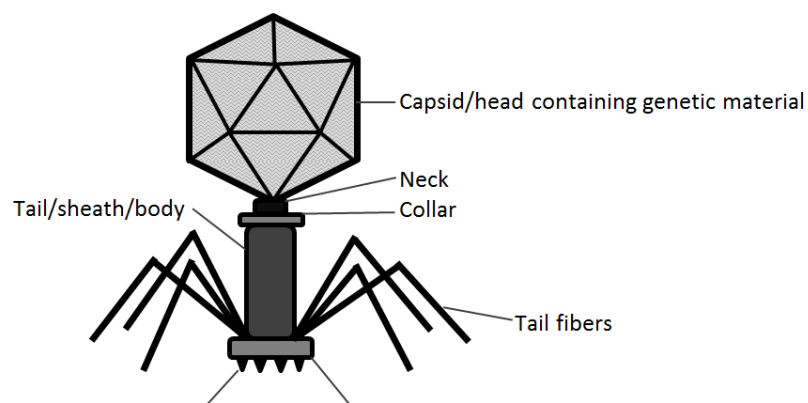
Figure 1.4- Ilustration of a tailed phage, from the *Caudovirales* order (Doss *et al.*, 2017)

The structure of a phage is composed of a head with a nucleic acid genome enveloped by a capsid, consisting on a single or double–stranded DNA or RNA. According to their life cycle, phages can be classified as virulent or temperate (Sieiro *et al.*, 2020; Yu *et al.*, 2016). Virulent phages have a lytic life cycle that starts when the phage binds to specific receptors found in the bacterial cell surface and injects its DNA into the cell. Inside the cell, the phage DNA is replicated, new progeny phages are assembled and then released due to bacterial cell lysis. These phages are able to start another round of infection (self-replicating capability) by targeting other pathogenic bacteria found in the same location. In the lysogenic life cycle, after injection of the genetic material, the phage genome is inserted into the host's chromosome and replicates with cell division (Figure 4). This phage is referred to as a prophage. Therefore, temperate phages do not immediately cause

bacterial cell lysis as it only occurs when there is an environmental change or when there are signs of stress (Doss *et al.*, 2017).
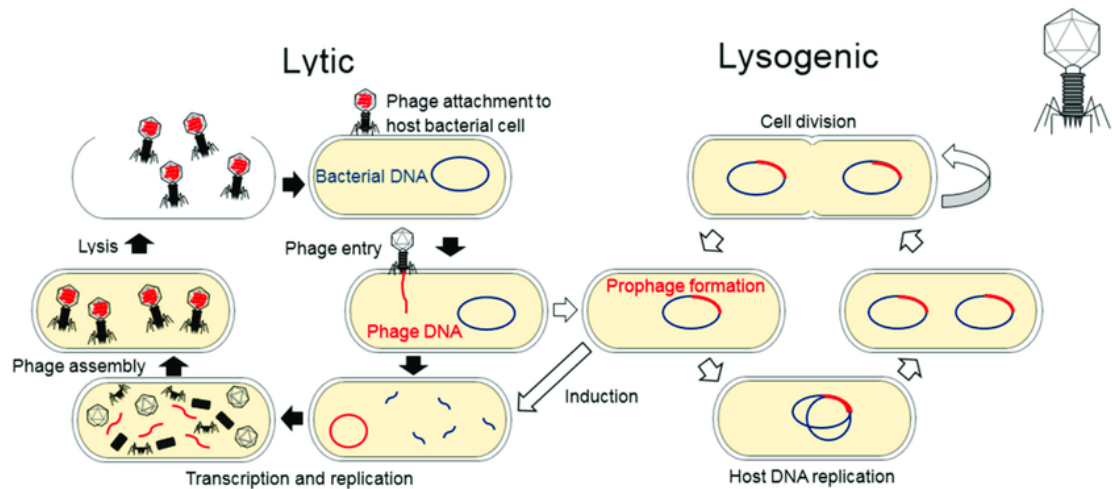
Figure 1.5- Lytic and Lysogenic cycle of bacteriophages (Batinovic *et al.*, 2019)

1.3.2. The use of phages for plant disease control

The first study developed on isolation of phages in plants was performed Mallmann & Hemstreet, (1924), the authors were able to inhibit the development of *Xanthomonas campestris* pv. *campestris* by filtering decaying cabbages. As mentioned above, the use of antibiotics replaced as well, in plants, the interest of using phages against pathogenic bacteria. Producers mostly started to use streptomycin and also copper-based products to inhibit the development of bacteria. However, over time, the use of these products led to bacterial resistance. Copper-based products can cause phytotoxicity when accumulated in the soil and, can be also toxic for plants and humans. These products can as well, affect the fruit itself by leaving toxic residues in them. Antibiotics on the other hand, can harm both pathogenic and beneficial bacteria for the plant (Sieiro *et al.*, 2020), thus being necessary to find different approaches. Bacteriophages can be a biological alternative to chemical products, with the benefit of controlling bacterial diseases that have no effective biological control method, since phages have the advantage of having no negative effect against animal or plant cells (Chan *et al.*, 2013; Gill & Hyman, 2010; Yu *et al.*, 2016). The ease of phage isolation, efficiency against biofilms and the capacity of self-replication are some of the advantages of using bacteriophages as a control method, as well as being environment friendly and non-toxic to eukaryotes (Sieiro *et al.*, 2020).

Through the years, a lot of studies have been taking place to characterize phages against plant diseases caused by phytopathogenic bacteria. Studies in fruit trees, citrus, tomato and potato are the most common performed with phages (Balogh *et al.*, 2010), that is the case of *Xanthomonas axonopodis* pv. *citri* , causal agent of asiatic citrus canker, phages were tested as a biocontrol for citrus canker and citrus bacterial spot and it was observed 59% of reduction in disease severity by using a phage cocktail (Balogh *et al.*, 2008). The control of bacterial spot on tomato, caused by *Xanthomonas campestris* pv. *vesicatoria* was also studied with phages to stop spot disease on tomato and pepper, in this study, besides decreasing the disease severity, there was an increase on total weight of the fruit by using phages (Flaherty *et al.*, 2000). Still within the *Xanthomonas* genus, the prevention of the disease of bacterial blight of granium, provoked by *Xanthomonas campestris* pv. *pelargonii* was also studied by using h-mutant phages that were able to reduce up to 75% of incidence (Flaherty *et al.*, 2001). *Erwinia amylovora*, the causal agent of fire blight that appears mostly in fruit trees, phages were able to reduced infection by 84% to 96% infection in studies with pear blossom by using the bacteria *Pantoea agglomeran*s as a carrier (Boulé *et al.*, 2011). In the case of *Dickeya solani,* the bacteria that causes soft rot and blackleg diseases on potato, *in vitro* assays demonstrated that phages stopped completely the growth of this pathogenic bacteria (Czajkowski *et al.*, 2014). Bacterial wilt, caused by *Ralstonia solanacearum* was inhibit by using phage and also application of phage with a surfactant (Silwet L-77) (Young *et al.*, 2012). *Pectobacterium carotovorum* that causes soft rot in several crops like potato and tomato, was reduced when treated with phage PP1 (Lim *et al.*, 2013).

In addition to phage-only treatments, the application of phage with integration of products already used for Psa control was also studied (Balogh *et al.*, 2010). Application of phages with acibenzolar-S-methyl was shown to suppress hypersensitive reaction on bacterial spot disease in tomato incited by *Xanthomonas campestris* pv. *vesicatoria* (Obradovic *et al.*, 2005) and also reduce of leaf blight of onion, caused by *Xanthomonas axonopodis* pv. *allii* (Lang *et al.*, 2007).

At the time, several phage biocontrol products are already available (Buttimer *et al.*, 2017). In the United States there are several products registered and approved by United States Environmental Protection Agency produced by OmniLytics Inc., such as AgriPhage, created to control tomato and pepper bacterial spot caused by *Xanthomonas campestris* pv. *vesicatoria* and also control *Pseudomonas syringae* pv. *tomato* (EPA, 2005), Agriphage – Fire Blight, to control *Erwinia amylovora* on apple and pear trees (EPA, 2018), Agriphage – CMM, to control tomato bacterial canker caused by *Clavibacter michiganensis* pv. *michiganensis* (OmniLytics Inc., 2019)

and Agriphage – Citrus Canker to control *Xanthomonas citri* pv. *citri* (OmniLytics Inc., 2018). In Hungary it was approved the use of Erwiphage, specific for *Erwinia amylovora* produced by Enviroinvest (Buttimer *et al.*, 2017; Erwiphage *et al.*, 2021) and lastly, in Scotland it was produced Biolyse, from APS Biocontrol Ltd, specific to control *Enterobacteriacea*, used to prevent soft rot on potatoes during storage (Buttimer *et al.*, 2017).

1.3.3. The use of phages on actinidia plants

Phages targeting *Pseudomonas syringae* pv. *actnidiae* have already been reported and characterized and are usually isolated from water, soil and leaves of Actinidia (Yu *et al.*, 2016). Since 2014, researchers from New Zealand and Italy, started to isolate and characterize phages to study their efficacy as a biological control method for the bacterial canker caused by Psa (Di Lallo *et al.*, 2014; Frampton *et al.*, 2014). Most of phages targeting Psa belong to *Myoviridae*, *Podoviridae* and *Siphoviridae* families from the *Caudovirales* order (Pereira *et al.*, 2021).

To test if the phages are efficient, host range and stability studies were executed. The host range is important to analyze how many strains the phage can cause lysis and also, in this case, if affects other bacteria present in kiwifruit plants. The host range also can help to analyze if another phage can complement other bacteriophage host range by creating a cocktail to infect Psa strains to increase their host range and be more effective (Flores *et al.*, 2020). Stability studies are also important to study phage capacity to different temperatures, pH and UV light (Yu *et al.*, 2016). After isolating phages and study their efficiency, researchers started to sequence phage genomes to understand their genomic features and find proteins that cause lysis and confirm phages to be lytic (Park *et al.*, 2018). Later, *in vitro* tests began to observe how much time was necessary to reduce the bacterial load of Psa and also assays with kiwifruit plants started to appear to confirm the previous *in vitro* results (Table 1) (Flores *et al.*, 2020). In Portugal, Pinheiro *et al.*, (2020) tested an already commercially available phage (phage ɸ6) to control Psa infection on *in vitro* and *ex vivo* assays.

Table 1.1 - Summary of *in vitro* and *in vivo* assays with targeted Psa in kiwifruit

Phages (taxonomy)	Procedure	Results	Reference
φPSA2 (*Podoviridae*)	Phage infected Psa strain at MOI of 0.01. Samples taken at intervals of 30 min, 2h and 24h	Time of death of Psa strain was approximately 155 min.	Di Lallo *et al.*, (2014)
KHUφ34 (*Myoviridae*) KHUφ38 (*Podoviridae*) KHUφ44 (*Myoviridae*) KHUφ59 (*Podoviridae*) KHUφ74 (*Podoviridae*)	Phage lysate was added at a MOI of 0.01. OD_{600} was measured for 80h.	Bacteriophage KHUφ38 showed lytic activity slightly later than KHUφ59 and KHUφ74, and their lytic activity increased during the first 24 h. Bacteriophages KHUφ34 and KHUφ44 did not show lytic activity until 24 h.	Yu *et al.*, (2016)
PPPL-1 (*Podoviridae*)	Phage (MOI= 0.01) was added to a bacterial suspension in the early exponential phase, and OD_{600} was measured at the designated time points.	The bacterial density was gradually reduced nearly to 0.1 for 12 h and then was slowly increased up to 80 h	Park *et al.*, (2018)
Phage Φ6 (*Cystoviridae*)	Bacterial inactivation by phage Φ6 at a MOI of 1 added to the bacterial suspension at exponential phase adjusted to a 0,7 at 600 nm. Bacterial and phage controls were collected at time during 24h.	Phage φ6 promoted a significant decrease in the concentration of both Psa CRA-FRU 12.54 and Psa CRA-FRU 14.10 strains for 24h.	Pinheiro *et al.*, (2020)
PN05 (*Myoviridae*) PN09 (*Myoviridae*)	Psa culture was diluted (1:100) and phages were added at MOIs 0.1, 1, 10 and 100. Bacteriolytic activity was measured at 600 nm at 1h intervals for 40h.	Psa was completely inhibited for 12h when treated with PN05 and 18h when treated with PN09 with MOIs 0.1, 1 and 10. At MOI 100, Psa was completely inhibited for 22h with PN05 and 26h with phage PN09.	Ni *et al.*, (2020)
CHF1(*Podoviridae*) CHF7(*Podoviridae*) CHF19(*Podoviridae*) CHF21(*Podoviridae*)	Kiwifruit leaf discs were placed in humidity chambers and inoculated individually with three drops of 10 µL of Psa. The phage cocktail was added two hours after Psa with a MOI of 10. Lytic activity was measured at 0,3 and 24h.	The cocktail of phages in equal proportion was able to reduce the bacterial load of Psa over leaves below the detection limit (20 UFC/mL) within 3 h post-infection (hpi), and remained undetected up to 24 hpi.	Flores *et al.*, (2020)
PPPL-1 (*Podoviridae*)	Leaves treated with phage resuspension. After 2h, the bacteria suspension was treated using the same method. Observation occurred during 7 days to 5 weeks.	The PPPL-1 phage application significantly protected the treated leaves with Psa, based on the reduction in visible symptomatic spots compared to the untreated one.	Song *et al.*, (2021)

1.4. Aims

Due to its great propagation capacity, its severe symptoms and also the economic and productive loss of kiwi fruit, it is necessary to find effective solutions to control Psa. Therefore, the main goal of this study is to develop an alternative strategy, based on bacteriophages for the control of Psa by isolate and characterize phages from Portuguese orchards. Select phages to apply in kiwifruit orchards infected with Psa. In the end, the goal is to have an efficient product for the biocontrol of one of the most dangerous phytopathogenic bacteria of Actinidia, Psa biovar3.

2. Material and Methods

2.1. Isolation and Characterization of Pseudomonas *syringae pv. actinidiae*

2.1.1.   Pathogen Isolation

For the isolation of *Pseudomonas syringae* pv. *actinidiae* samples of branches, leaves, sepals, petals, stems and flower buds of *A. deliciosa* plants with Psa symptoms were collected during the growing season of 2019, 2020 and 2021 in Portuguese kiwifruit orchards in the Minho Region, namely the company KiwiGreenSun, SA, Braga, Cabeceiras de Basto and Póvoa de Lanhoso. A necrotic portion was cut out from each sample, disinfected with 70% ethanol and added to sterile distilled water for 5 minutes. Plant tissues were macerated with the help of a scalpel in sterile distilled water and left to stand for 5 minutes to release the bacteria from the tissues until obtaining a suspension with the bacteria (Moura *et al.*, 2015). Bacterial suspension of each sample was inoculated in King B medium modified with boric acid, cephalexin and cycloheximide (Mohan & Schaad, 1987) and incubated for 48 hours at 28°C. 55 colonies with known Psa characteristics were streaked into King B medium to obtain pure colonies, which were preserved at -20°C and -80°C, for further characterization (Garcia, 2015) .

2.1.2.   Morphological characterization

In the characterization of the bacterial isolates, the colony size, shape and fluorescence in King B medium were taken into account. Oxidase tests were performed and the 3% Potassium hydroxide (KOH) method (Suslow *et al.*, 1982) was used to characterize Gram stain reaction (Moura *et al.*, 2015).

2.1.3.   Molecular characterization

For the identification and molecular characterization of isolates, bacterial suspensions were prepared from pure cultures with 48 hours using the "colony PCR" method, which were kept at -20°C and later used in PCR reactions.

For the identification of Psa, the Duplex-PCR technique was used (Gallelli *et al.*, 2011). A PCR mixture (Table 2.1) was prepared with two Psa-specific primer pairs: KN-F (5'-

CACGATACATGGGCTTATGC-3 '), KN-R (5'-CTTTTCATCCACACACTCCG-3') (Koh & Nou, 2002) and AvrDdpx- F (5'-TTTCGGTGGTAACGTTGGCA-3 '), AvrDdpx-R (5'-TTCCGCTAGGTGAAAAATGGG-3') (Gallelli *et al.*, 2011). In each PCR reaction A negative control (sterile ultrapure water) and a positive Psa control (CFBP 7286) were systematically included. DNA amplifications occurred in a GeneAMp PCR thermocycler System 2400 (Perkin Elmer®) with the programming indicated in the Table 2.2.

Table 2.1- PCR mix for amplification of DNA fragments (Duplex PCR KN-F / KN-R and AvrdDpx-F / AvrdDpx-R)

PCR Mixture	Volume per reaction (µL)
Sigma ReadyMix RedTaq*	10
Primer KN-F	1,25
Primer KN-R	1,25
Primer AvrdDpx-F	1
Primer AvrdDpx-R	1
Sterile MilliQ Water	5,5
DNA	5
	25 (Total)

*REDTaq® ReadyMixTM PCR Reaction Mix with MgCl2, Sigma-Aldrich.

Table 2.2- PCR program for DNA amplification using KN-F / KN-R and AvrdDpx-F / AvrdDpx-R primers

Number of cycles	Temperature	Time
1	95 °C	3 min
30	94 °C	30 s
	63 °C	45 s
	72 °C	50 s
1	72°C	5 min
1	4°C	∞

The amplified DNA fragments were separated by electrophoresis on 1.5% (w/v) agarose gel in 1x TBE to which 2µL of GelRed® (Biotium) The wells were loaded with 8µL of the DNA

sample to be analyzed, added of 2μL of Blue/Orange 6X Loading marker Dye (Promega). To reference the size of the amplified bands the gel was loaded with 5 μl of 100 bp ladder (BIORON). Electrophoresis was carried out at 145 V for 45 minutes. The results were observed in the transilluminator under UV light, where it was possible to observe the amplification of both the fragments of 492 bp and 226 bp for some isolates, which were thus identified as *P. syringae* pv. *actinidiae.* The gel images were saved in digital format for further analysis.

Psa selected strains were additionally characterized by BOX - PCR, using the primer BOXA1R (5'-CTA CGG CAA GGC GAC GCT GAC G-3 ') as described by Louws *et al.* (1994). The composition of the PCR mix and the amplification program are described in Tables 2.3 and 2.4, respectively.

Table 2.3- Mixture for amplification of DNA fragments by BOX-PCR (Vaz, 2017)

PCR Mixture	Volume per reaction (μL)
Sigma ReadyMix RedTaq*	12,5
Primer BOXA1R	5
Sterile MilliQ Water	5
DNA	2,5
	25 (Total)

* REDTaq® ReadyMixTM PCR Reaction Mix with MgCl2, Sigma-Aldrich.

Table 2.4- PCR program for amplification of repeated sequences using the BOXA1R primer (Louws *et al.*, 1994)

Number of cycles	Temperature	Time
1	95 °C	7 min
	94 °C	1 min
30	53 °C	1 min
	65 °C	8 min
1	65°C	15 min
1	4°C	∞

The amplified DNA fragments were separated by electrophoresis on 2% agarose gel in 0.5x TBE and GelRed® (Biotium) The gel was loaded with 5 μl of 100 bp ladder and the electrophoresis

was carried out at 100 V for 1h30 min. The results were checked using a transilluminator under UV light, and images saved in digital format for further analysis.

2.1.4. Phenotypic characterization

For the phenotypic characterization of bacteria, BIOLOG GEN III Microplates (MicroplateTM, Biolog) were used.

Twenty portuguese isolates previously identified as Psa by duplex-PCR were used. Additionally, CFBP 7286, an Italian Psa biovar 3 reference strain, as well as P84, a Portuguese Psa biovar 3 strain previously referred in prior publications (Garcia *et al.*, 2018; Moura *et al.*, 2015), the pathotype stain of Psa CFBP 4909ᵀ (Japanese, biovar 1), and *Pseudomonas syringae* pv. *actinidifoliorum* CFBP 7812 (reclassification of Psa biovar 4) were also included in this analysis. Suspensions of pure cultures each isolate were prepared using the fluid IF-A (Biolog), the concentration were standardized uising a Biolog Turbidimeter and 100 µl of the bacterial suspension was dispensed in each well of the Biolog GEN III microplate. The plates were incubated at 28ºC and the optical density (590 nm) were read after 24, 48 and 72 hours, using the Biolog GEN III Micro Station™ ID System and the software MicroLogTM. Additionally, the optical density was read in a ASYS UVM 340 microplate reader (Hitech GmbH, Austria). The results of physiologic and biochemical characteristics of bacterial strains obtained with Biolog GEN III microplates, were analyzed by PAST 3 software (Øyvind Hammer, Natural History Museum, University of Oslo) and were compared using the correlation coefficient and the unweighted pair-group method using arithmetic averages (UPGMA) (Unweigted Pair Group Method using arithmetic Averages) (Sneath and Sokal, 1973).

2.1.5. *Pseudomonas syringae* pv. *actinidiae* Growth Curve

The different phases of the bacterial growth were assessed *in vitro* using one of the Portuguese Psa strains, named P84.   This strain was grown overnight, and then the culture was diluted with a dilution factor (DF) of 1:50 by adding 500 µL of the overnight grown culture on 25 mL of Tryptic Soy Broth (TSB) and incubated at 28ºC under agitation (120 rpm). The OD was measured at 600 nm every hour since time zero until 9 h of incubation, and then it was measured

after 24 h to 26 h. Simultaneously, 50 μL of the bacterial suspension was taken in every time point and serial dilutions (1:10) were made in NaCl 0,9%. After, 10 μL of each dilution was placed in a petri dish with Tryptic Soy Agar (TSB + 1.2% of agar) and allowed to run down the plate to create a drop effect in order to allow the quantification of colony forming units (CFUs) after overnight incubation at 28°C for 48h. These data allowed the construction of a calibration curve OD vs. CFUs.

2.2. Isolation and Characterization of phages targeting Psa

2.2.1. Phage extraction

Leaves, flowers, flowers buds, stems, weed, and soil samples from kiwifruit orchards were used for phage extraction. Each sample was placed in stomacher bags with 30 mL of distilled sterile water. The samples were homogenized in the Seward Stomacher 400 for 120 seconds and the mixture was filtered through 0.22 μm nylon membrane filter and collected into 15 mL falcon tubes.

In leaf samples, only one leaf was added to each stomacher bag; flowers and buds were added 3 per bag. For soil samples, 10 g of soil was weighed and placed in a stomacher bag and. After homogenization, the samples were centrifuged at 5,000 rpm for 10 minutes, filtered through 0.22 μm nylon membrane filter and collected into 15 mL falcon tubes. For an initial screening of the presence of phages in the homogenized samples, a double layer of soft TSA (TSB + 0.6% (w/v) of agar) was mixed with 1 mL of filtrate and 300 μL of Psa bacterial suspensions (P84 and CFBP 7286) in TSA petri dishes. The plates were incubated at 28°C for 24h.

2.2.2. Phage isolation, propagation and titration

After checking the presence of phage plaques on the extracts, phages were isolated using the enrichment procedure with Psa strains CFBP 7286 and P84 as possible hosts. For this, 6 mL of each extract collected from kiwi leaves, flowers, buds, trunks, soil and weeds were mixed with 15 mL of double concentrated TSB and also 25 μL of both CFBP 7286 and P84 cultures. The cultures were incubated at 28°C, 120 rpm for 24h and then centrifuged (9,000 × g, 4°C for 10 min), filtered and the spot test was performed by placing a 10 μL drop on a bacterial lawn (previously prepared by mixing 100 μL of bacterial suspension with 3-5 mL of TSB top-agar (TSB

+ 0.6% (w/v) of agar) in a TSA plate). The plates were incubated at 28°C for 24h and after, the presence of lysis zones was analyzed. If an inhibition halo was observed in the plates, individual phage plaques were then isolated and purified using sterile toothpicks and papers until single plaque morphology was observed (Figure 2.1.) (Azeredo *et al.*, 2014).
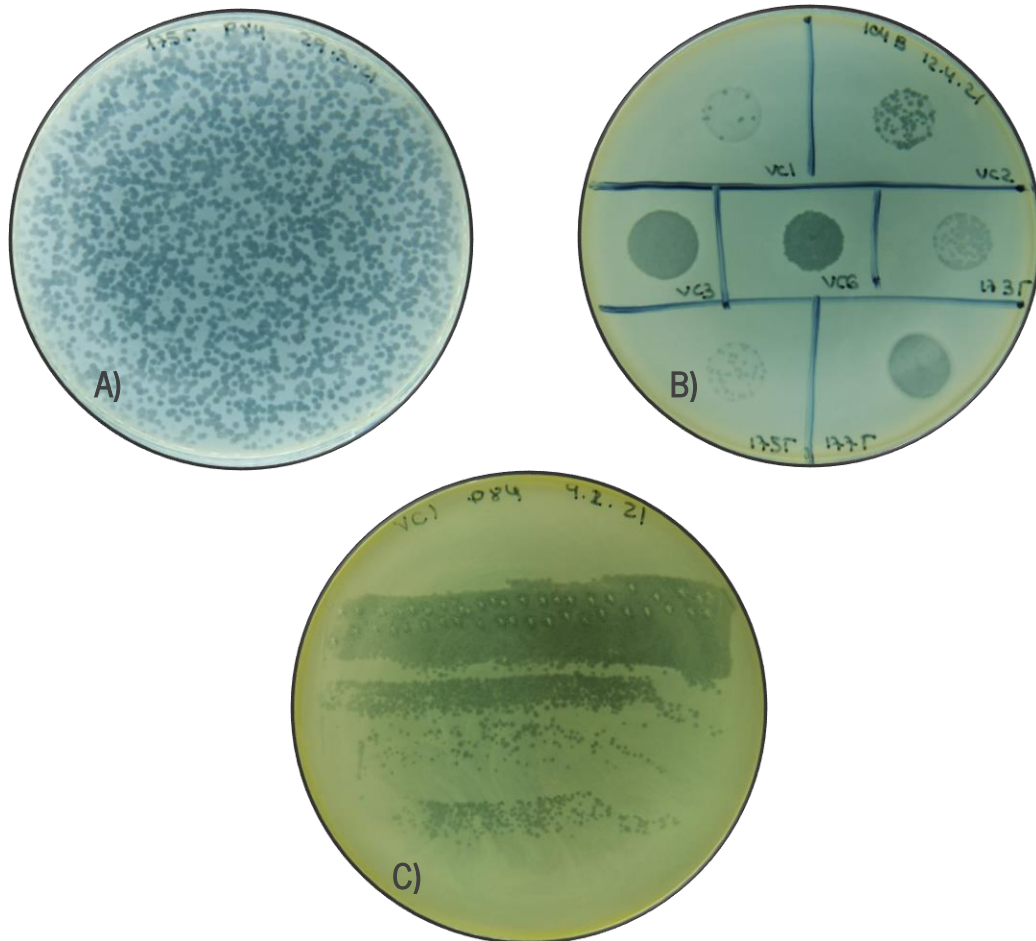
Figure 2.1– A) First test for phage observation in plant tissue extracts; B) Spot test after enrichment procedure; C) Phage isolation technique to obtain phage plaque purification.

After isolation, phage production was performed according to previously described protocols with minor modifications (Azeredo *et al.*, 2014). Briefly, for each phage, a well isolated phage plaque was picked with a toothpick to TSA plates containing the lawns of the host P84 strain and then spread throughout the plates with paper strips. The petri dishes were incubated at 28°C for 24h and, after incubation, 2.5 mL of Saline Magnesium Buffer (SM Buffer) (5,8 g/L NaCl, 2 g/L $MgSO_4$, 50 mL/L 1 M Tris-HCl pH 7.5) were added to each petri dish and incubated at 4°C with agitation (80 rpm) for 5-6h.

After, the SM Buffer and top agar were collected, centrifuged (9000 x g, 4°C for 10 min) and the supernatant was recovered and filtered (0.22 µm). The phage suspension was stored at 4°C until further use.

The phage titration was performed using the double agar overlay technique. Briefly, serial dilutions of phage stock solutions were made in SM Buffer. Subsequently, 10 µL of each phage dilution was placed in a TSA plate containing the host bacterial lawn to create a drop effect. The plates were incubated at 23°C for 24h and the number of PFUs were counted.

To calculate the phage titre, the following equation was used:

Equation 2.1.- Bacteriophage titer

$$\text{Bacteriophage titer (PFU per mL)} = \frac{\text{Nr. of bacteriophage plaques formed} \times \text{Diluition factor}}{\text{Volume of bacteriophage sample (mL)}}$$

2.2.3. Host Range

The host range of the isolated phages was evaluated using a collection of 41 Psa strains previously isolated and identified. One drop (10 µL) of each phage was spotted on the lawns of the different bacterial isolates. The petri dishes were incubated at room temperature (23°C) for 24h and the presence of an inhibition halo for each phage was analyzed. Later, 10 µL of decimal serial dilutions of each phage were tested on the same bacterial lawns, with phage titers ranging from 10^3 to 10^6 PFU/mL, in order to assess if the lysis observed could be caused by Lysis from without (LFW). This observation was done after overnight incubation of the plates at 23°C.

The isolated phages were morphologically characterized by Transmission Electron Microscopy (TEM) using a procedure previously described (Melo *et al.*, 2014; Pires *et al.*, 2021).

2.2.4. Phage growth parameters

The phage growth parameters were evaluated through one-step growth curves (OSGC) (Di Lallo *et al.*, 2014; Liu *et al.*, 2021; Ni *et al.*, 2021). The host strain P84 biovar 3 was grown in TSB until the cells reached the exponential phase (OD_{600} = 0.3 to 0.5). Then, the bacterial suspension

was centrifuged (7,000 x g, 4 °C, 5min), the pellet was resuspended in 5 mL of fresh media and 5 mL of phage were added to obtain a multiplicity of infection (MOI) of 0.01. The culture was incubated with agitation for 5 minutes to allow the phages to adsorb to the host cells and after, it was centrifuged (7,000 x g, 4 °C, 5min), the supernatant was discarded and the pellet was resuspended with 10 mL of fresh TSB medium. One sample was immediately taken (t0) and the culture was then incubated at 26°C with agitation of 120 rpm. Samples were taken at 20 minutes intervals until 180 minutes, and serial dilutions were performed to enumerate the number of PFUs in each time point.

2.2.5. Phage Stability

The thermal stability of the phages was assessed by incubating 10^8 PFU/mL of each phage at different temperatures: -20°C, 4 °C (control), 28 °C, 37 °C, 50 °C and 60°C for 24 and 48 hours. Similarly, the stability of phages to pH was evaluated using a universal buffer (150 mM of KCl, 10mM of KH_2PO_4 and 10mM of $C_6H_5Na_3O_7$) with different pH values: 1, 3, 5, 7 (control), 9, 11 and 13. Phages (10^8 PFU/mL) were incubated in each pH at 4°C for 24 and 48 hours. All tests were performed in triplicate.

To study the phages' stability to UV light, a protocol by Yu *et al.* (2016) was followed with slightly modifications. Phage aliquots with 10^8 PFU/mL in SM Buffer were incubated into a 96 well microtiter plate and placed over a 366 nm UV light. Samples were taken every 15 minutes for 3 hours.

After incubation under the different conditions described above, serial dilutions of phages were made and the PFUs were evaluated. All the assays were carried on two and three independent assays performed in duplicate.

2.2.6. Phage DNA extraction

For phage DNA extraction, 1 mL of phage lysate was transferred to a 2 mL eppendorf tube and then added 12.5 µL of 1M $MgCl_2$ and mixed gently. Then, 1 µL of DNAse (10 mg/mL) and 1 µL of RNAse A (100 mg/mL) was added to the lysate, vortexed and incubated at room temperature for 1 hour. After incubation, of the following solutions were sequentially added: 40 µL of 0,5M of EDTA, 5 µL of Proteinase K (10 mg/mL) and 50 µL of 10% SDS; then, the mixture was vigorously vortexed and incubated overnight at 55°C.

After overnight incubation, 500 µL of the mixture were transferred into two 1.5 mL microcentrifuge tubes and 500 µL of phenol were added. This mixture was centrifuged (13,000× g, 10 min at room temperature) and then, the aqueous phase was transferred to a new tube and added 250 µL of chloroform and 250 µL of phenol followed again by centrifugation (13,000× g, 10 min at room temperature). The aqueous phase was extracted again and 500 µL of chloroform were added and centrifuged with the same conditions mentioned previously. The top aqueous layer above the white interphase was recovered and the DNA was precipitated by adding 1mL of absolute ethanol and 50 µL of 3M sodium acetate solution. The samples were placed on ice for 30 minutes to help with precipitation. After, the samples were centrifuged (15 minutes at 14,000 × g at 4°C) and the pellets were washed with 500 µL of 70% (v/v) of ethanol. After a new centrifugation (14,000 × g, 4°C, 5 min) the ethanol was removed and the pellets were air dried for approximately 2 hours. After, the pellets were dissolved in 5 µL of sterile dH_2O and the DNA samples were stored at -20°C until further analysis. To verify if the phage DNA extraction was successful, the DNA concentration was measured using a NanoDrop and then the samples were loaded through an agarose gel (1% (w/v)) electrophoresis with a sample mix of 1.5 µL of DNA, 5 µL of H_2O and 2 µL of Loading Dye. In the agarose gel it was also added 5 µL of 1kb marker (Grisp).

2.2.7.   Genome alignment and annotation

The phages genomic DNA was sequenced in an external laboratory. The obtained data was assembled and annotated using Geneious Prime software, myRAST, and online platforms, such as Phobius for transmembrane domains detection, SignalP 4.1 server for signal peptides, Promoter 2.0 Prediction Server, Arnold - FInding terminators for detection of Rho-Independent Terminators and Aragorn for tRNA detection.

BLASTn was used to compare the genome to the NCBI database. Manual annotation was performed by using BLASTp to compare Geneious Prime predicted ORFs to the GenBank protein database.

2.3. *In vitro* phage infection assays

2.3.1.   *In vitro* infection assays in culture medium

To assess the in vitro antibacterial activity of phages, the host strain P84 was grown in 25 mL of TSB for 24h at 26°C with agitation (120 rpm). Bacterial culture was adjusted to 0.4 (OD_{600}) with fresh medium and the bacterial suspension was divided in volumes of 15 mL in two 50 mL flasks. One of the cultures was infected with phage at a MOI = 1 and the other was used as a control (no phage). Both cultures were then incubated again at 26°C and 120 rpm. Samples were taken in duplicate after 0, 2, 4, 6, 24, 27, 30 and 48h of incubation for OD measurements and quantification of PFUs and CFUs, through the drop technique already described (2.2.2. Phage isolation, propagation and titration). PFU's were observed after 24h incubation at 23°C and CFUs were counted after 48h incubation.

2.4. *In vivo* phage infection assays

2.4.1.   *In vivo* infection assays in Actinidea leaf discs

In vivo assays using leaf discs obtained from healthy kiwifruit plants (*Actinidea deliciosa* "Hayward") were performed according to a protocol described by Flores *et al.* (2020) with slightly alterations. This assay was performed in 3 different groups: two groups infected with (Psa strain

P84 + phage 177T; P84 + phage VC3). Leaf discs only infected with Psa were used as a control group. Each group correspond to four leaf discs on a humidity chamber (Figure 2.2). Kiwi leaf discs with 2 cm diameter were disinfected with sodium hypochlorite 1% (v/v) and washed two times with sterile distilled water. Then, the four leaf discs were placed on sterile humidity chambers, which are formed by cotton wrapped with filter paper, soaked in 25 mL of sterile distilled water in glass petri dishes. Each leaf disc was inoculated with three drops of 10 µL of Psa P84 (10^8 CFU/mL). Each phage was added to its correspondent group, two hours after inoculation with Psa, with a MOI =1. All humidity chambers were incubated at 20°C with relative humidity at 70% and with a photoperiod of 14h. One disk leaf inoculated was taken at the different time points: 0, 3, 24 and 48h post-infection. To quantify the bacterial and phage loads, leaf discs were homogenized with 1 mL of SM Buffer, followed by serial dilutions and plated on TSA medium (for CFU counts) or on bacterial lawns formed on TSA medium (for PFU counts). All the assays were carried out in biological triplicate.
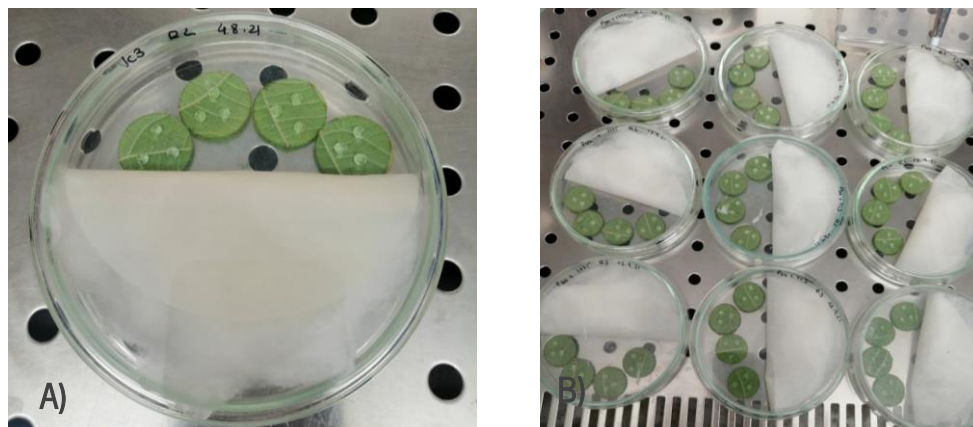
Figure 2.2- Humid chambers. A) Humid chamber with leaf discs inoculated with strain P84 at 10^8 CFU/mL. B) Humid chamber of all groups in triplicate.

2.5. Phage infection assays on plants

Preliminary plant infection assays were carried out in 2-year-old healthy kiwi plants (Flores *et al.*, 2020). Micro-lesions were created (Song *et al.*, 2021) and then, one of the leaves was inoculated with 2mL of P84 Psa suspension (10^8 CFU/mL) with a syringe on the adaxial and abaxial part. The leaf was covered with a plastic bag to retain the humidity and induce the proliferation of the bacteria. On another leaf, the same bacterial suspension and also a phage solution with phage

177T a MOI=1 was inoculated on both adaxial and abaxial part of the leaf, which was also covered with a plastic bag. Plants stayed at a photoperiod chamber with controlled temperature of 20°C and relative humidity of 70%. Observations of both leaves' evolution were performed every week.

2.6. Statistical analysis

GraphPad Prism 9 was used for statistical analysis, which included a two-way repeated measures analysis of variance (ANOVA) with Bonferroni post hoc testing. The data is provided as a mean with a standard deviation. For P-values less than 0.05, differences between samples were considered statistically significant.

3. Results & Discussion

3.1. Isolation of *Pseudomonas syringae* pv. *actinidiae*

After collecting a diverse number of samples, a total number of 238 bacterial isolates were obtained, and it was possible to isolate 55 *Pseudomonas syringae* pv. *actinidiea* (Psa) strains from stems, leaves, sepals, petals and flower buds of kiwifruit plants during 2019, 2020 and 2021. Most of the bacterial strains were isolated from an orchard in Briteiros, Guimarães, but some isolates were also collected from orchards in Braga, Famalicão and Póvoa de Lanhoso (Annex A). Besides the morphology of the bacterial isolates, all the Gram-negative and oxidase-negative strains were tested by Duplex-PCR to obtain its identification.

3.1.1. Molecular identification and characterization

The molecular identification of the bacterial isolates was performed using the two sets of primers: KN-F, KN-R designed by Koh and Nou (2002) and AvrDdpx-F, AvrDdpx-R that were previously described by Gallelli *et al.* (2011). In the presence of Psa, these primers will lead to the amplification of two DNA fragments of 492 bp and 226 bp, allowing a fast identification of the isolates obtained in the orchard as Psa (Figure 3.1).
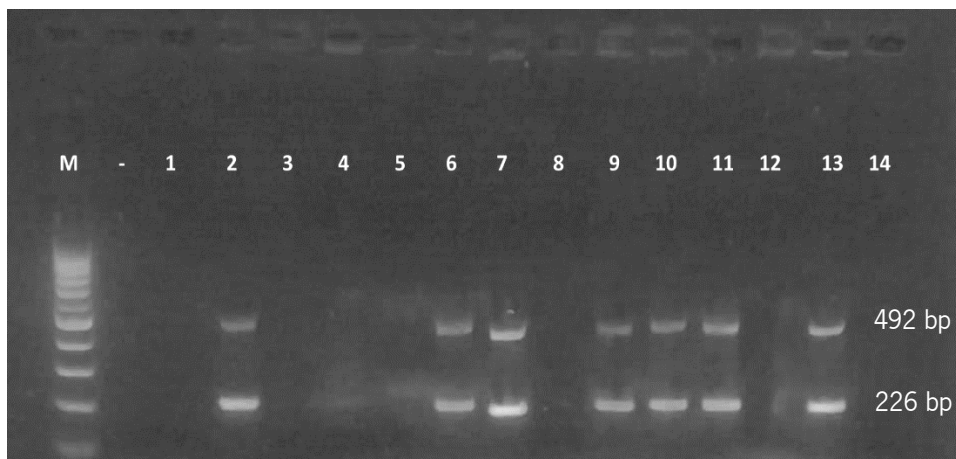
Figure 3.1- Example of a result obtained from Duplex-PCR using a few Psa strains with primers KN-F/R and AvrdDpx - F/R. M: Molecular marker (100bp plus DNA Ladder, BIORON), (-): negative control (Milli-Q water + PCR mix), 1 – 14: bacterial isolates collected from kiwi leaves from

Briteiros, Guimarães 1: 101F, 2: 102F, 3: 103F, 4:105F, 5: 106F, 6: 107F, 7: 108F, 8: 109F, 9: 111F, 10: 112F, 11: 113F, 12: 114F, 13: 115F and 14: 116F.

The sets of primers KN-F/R and AvrdDpx-F/R are specific for the detection of Psa and so, the simultaneously amplification of the two DNA fragments is a confirmation that the studied isolates are in fact Psa (Table 3.1).

Table 3.1- Total number of strains isolated and total number of strains identified as Psa by Duplex-PCR in different structures of Kiwifruit plants.

Plant Structure	Total n° of bacterial isolates	N° of Psa Isolates (Duplex – PCR)
Peduncle	2	2
Stalk	1	1
Branches	20	5
Bud	8	5
Sepal	25	10
Stamen	19	1
Petal	24	1
Leaf	103	30
Compost	24	0
Trunk	12	0
Total	238	55

Psa isolates were also characterized by BOX-PCR. BOX is a repetitive element used for molecular typing, a method used on Repetitive element-based PCR (Rep-PCR), that has been widely used to analyse the strain-specific patterns produced by PCR amplification of repetitive DNA elements found inside bacterial genomes. BOX elements are mosaic repeating elements made up of three subunit sequences in various combinations that are used for molecular typing. BoxA, boxB, and boxC are the three subunit sequences, and they are 59, 45, and 50 nucleotides long, respectively (Bilung *et al.*, 2018).

BOX-PCR was performed using the BOXA1R on Psa selected strains isolated from different sources and orchards in 2019 to analyze the different patterns among the isolates. The reference

strain CFBP7286 (Biovar 3) and the Portuguese P84 (Biovar 3) strain, isolated in 2013, were also included (Figure 3.2).
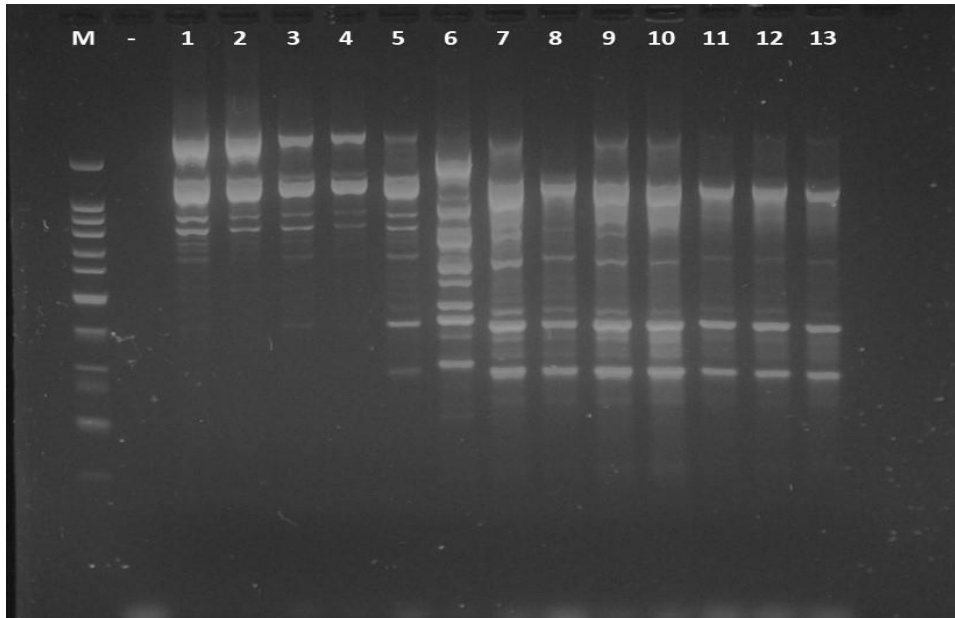
Figure 3.2- DNA amplification obtained with BOXA1R primer. M: Molecular Marker (100bp plus DNA Ladder, BIORON), (-): negative control (MilliQ water + PCR mix) 1: Psa-CFBP 7286, 2: Psa-P84, 3: 117P, 4:102F, 5:107F, 6:104S, 7: 106S, 8:388E, 9:103B, 10:104B, 11:3 (Peduncle, Cabeceiras de Basto), 12:21 (Leaf, Braga) and 13:23 (Leaf, Póvoa de Lanhoso).

According to figure 3.2, it is possible to observe several amplification patterns among samples. It is clear to see that the first four isolates (1-4) have the same profile as the reference strains CFBP7286 (1) and P84 (2), indicating their similarity. The last three isolates (11-13) all had the same pattern, although isolated from different orchards. With the exception of sample 6, which displays amplifications of bands of slightly varied sizes, there are similarities between the isolates in general. However, fading bands can be seen in samples 1, 2, 3, and 4, which might generate a pattern similar to the other isolates. The amount of DNA of each sample used to do the PCR might cause faded bands. Bacterial suspensions with the same optical density (OD_{600}=0.5) were always used, but the amount of DNA in each suspension could not be determined. As a result, the difference in electrophoresis between fading bands and more visible bands may represent differing quantities of DNA in the sample.

According to the study by Garcia (2015), who tested several Psa populations from different countries and also a selection of Psa strains from the Entre Douro e Minho region, it was possible to verify that the populations differ from each other, and the same happens within the same population. This analysis highlights the existence of variability within the Portuguese population of Psa, in the same way that occurs in this study. These variations reveal that repetitive sequences can be dispersed throughout the genome.

3.1.2. Phenotypic characterization by Biolog GEN III

Biolog GEN III is a method for obtaining phenotypic analyses and evaluating each strain's physiological characteristics, providing a reliable identification (Woźniak *et al.*, 2019). The Biolog method is based on measurements made on carbon substrates (Stefanowicz, 2006). The System Biolog was used to determine the ability to utilize carbon sources (sugars, alcohols, amino acids, and organic acids), physiological qualities (salts, pH, and tolerance to lactic acid), reducing power, and chemical sensitivity (Moura *et al.*, 2015). The usage of carbon sources is identified by an increase in the well's cell respiration, which results in an irreversible reduction of the tetrazolium dye and the formation of a purple color. Biolog profiles obtained for three Psa strains used in this study are presented in Figure 3.3. Biolog Microplate Gen III layout is presented on Annex B.

115S	CFBP7286ᵀ	P84
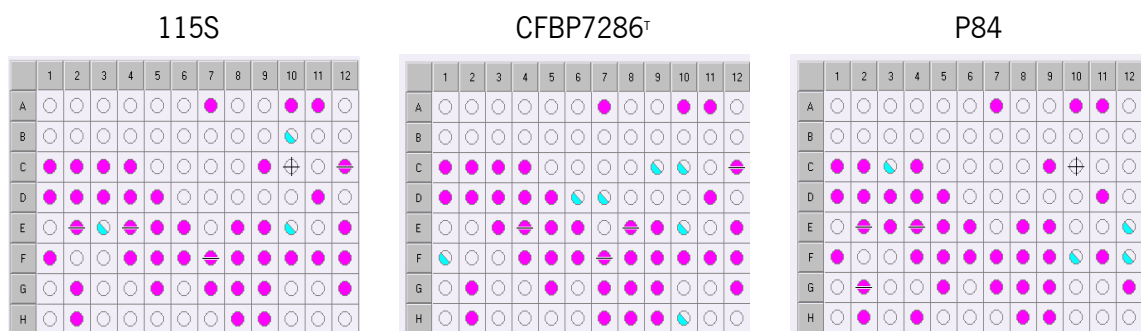
Figure 3.3- Biolog GEN III patterns: 115S - Psa strain isolated from sepals samples in 2019; CFBP7286 - Italian biovar 3 reference strain; P84 - biovar 3 strain isolated in Portugal in 2013.

The carbon source utilization tests in columns 1 through 9 are compared to the negative control well, A-1. All wells that resemble A-1 should be classified as "negative" (-) and all wells that are purple should be classified as "positive" (+). Wells with a very faint tint or little purple specks or clusters should be rated as "borderline" (\). The chemical sensivity experiments were conducted

in columns 10 to 12 and compared to a positive control, A-10. All wells with less than half the color of the A-10 well and considerable sensitivity to the inhibitory chemical are regarded "negative" (-) for growth. All other wells that have a normal or near-normal purple hue (like well A-10) are classified as "positive" (+). If the interpretation is unclear, it's recommended to score the well a "borderline" rating (\) (Biolog, 2008).

In this study it was possible to observe that all the Psa strains isolated display very similar patterns. Most of the strains were able to use different carbon sources such as Sucrose, α-D-Glucose, D-Mannose, D-Fructose, D-Galactose, Inosine, D-Sorbitol, D-Mannitol, D-Arabitol, myo-Inositol, Glycerol, Glycyl-L-Proline, L-Arginine, L-Aspartic Acid, L-Glutamic Acid, L-Pyroglutamic Acid, L-Serine, Pectin, D-Gluconic Acid, D-Glucuronic Acid, Glucuronamide, Mucic Acid, Quinic Acid, Methyl Pyruvate, Citric Acid, D-Malic Acid, L-Malic Acid, Bromo-Succinic Acid, y-Amino-Butryric Acid, Acetic Acid and Formic Acid, confirming the similarity between Psa isolates. However, the strains varied in their ability to use, L-Alanine, D-Glucose-6-PO4, D-Fructose-6-PO4 and β-Hydroxy-D, L-Butyric Acid. Otherwise, a few strains were sensitive to Rifamycin SV, D-Serine, Vancomycin and Potassium Tellurite. When compared to the results of Moura et al., 2015 study, which was based on the isolation of Psa strains isolated in Portugal's Entre e Douro e Minho region in 2013 and 2014, these patterns are similar. The same was described by Flores *et al.* (2018) on Chilean strains, however these were more sensitive to Aztreonam, Nalidixic Acid, and Fusidic Acid. Despite the phenotypic variability observed between strains analyzed in this study, all the Portuguese strains isolated in 2019 and 2021 were identified as Psa.

The result of the analysis of 95 phenotypic tests of the 20 strains tested, using Biolog Gen III microplates, generated the dendrogram shown in Figure 3.4, using the Past3 program.

The results of the analysis of 95 physiologic and biochemical characteristics tested by Biolog GEN III, generated the dendrogram present in Figure 3.4. For a similarity value of 0.88 there are 2 fena and 2 strains grouped together. The fenon 1, group of 7 portuguese Psa strains (6 isolated in 2019 in Guimarães and P84). The Fenon 2, group of 14 portuguese Psa strains isolated in Cabeceiras de Basto, Braga, Póvoa de Lanhoso and Guimarães in 2019 and 2021, and the Italian Psa biovar 3 reference strain, CFBP 7286. Psa biovar 1 (CFBP 4909[T]), the Japanese reference strain, and *Pseudomonas syringae* pv. *actinidifoliorum* (CFBP 7812), remain not grouped.
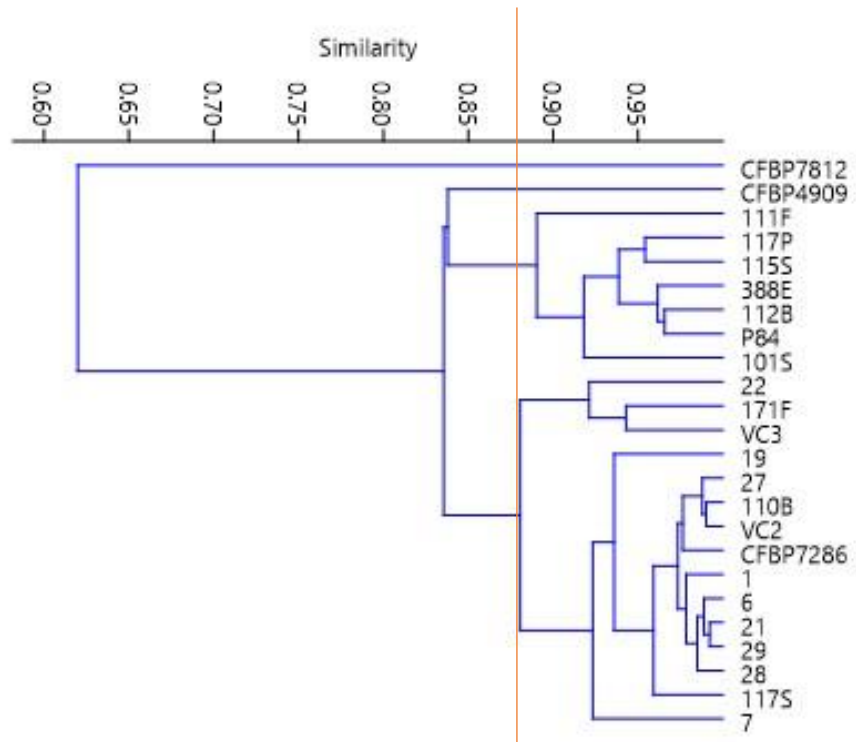
Figure 3.4– Dendrogram of phenotypic distances between twenty Psa Portuguese strains isolated in this study in 2019, and 2021 (1, 6, 7, 19, 21, 22, 27, 28, 29, 101S, 110B, 111F, 112B, 115S, 117P, 117S, 171F, 388E, VC2, VC3). P84- Portuguese Psa strain biovar 3 isolated in 2013; CFBP7286 - Italian reference strain of Psa biovar 3, CFBP4909[T] – Psa reference strain (biovar 1) and CFBP7812 – *Pseudomonas syringae* pv. *actinidifoliorum* (Psaf).

3.1.3. Psa growth curve and calibration curve

Microorganism growth curves may be used to determine in which development phase a microorganism is according to the incubation time. The latent phase, or most known as Lag phase, is determined by a transition period of adaption of the cells to the culture medium and to new nutrients. Because the cells do not instantly proliferate in a fresh medium, the number of cells does not vary much during this phase (Robinson *et al.*, 1998; Tortora *et al.*, 2013). The exponential phase, or also mentioned as Log phase, is the most metabolically active stage of the culture, when cells begin to divide and enter a phase of growth or logarithmic rise - it is the time when cell reproduction is most active. Because the generation time is constant during this period, the

logarithmic representation creates a straight line. During this phase, the nutrients in the medium begin to decrease once a significant number of cells have formed, and hazardous residues from the cells' metabolic activities begin to accumulate in the medium. These variables cause a slow down of the multiplication rate, resulting in a drop in the number of new cells while the number of dead cells rises, resulting in an equilibrium period known as the stationary phase. The last phase is marked by a large number of dead cells at a time when cell multiplication is rare, signaling the end of the equilibrium period and the start of a logarithmic fall known as the cell death phase. This stage lasts until the microbial population is significantly reduced or extinct (Tortora *et al.*, 2013). To better understand the different phases of P84 strain, a growth curve was performed and is presented in Figure 3.5.
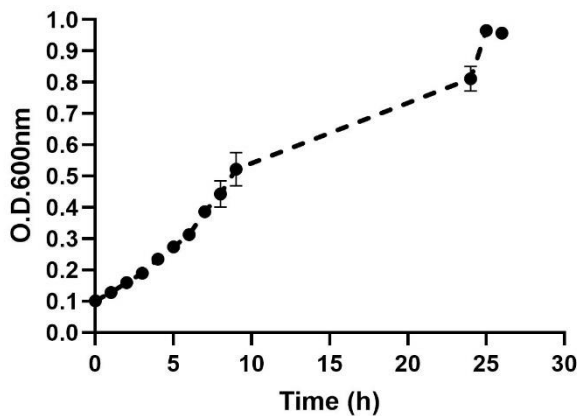
Figure 3.5- Growth curve of P84 strain (Psa biovar 3)

Figure 3.5 shows the growth curve of Psa during 26 hours at 28°C. Although the bacterial growth at the beginning is slow, it is not possible to clearly observe the lag phase and determine the latency period. As this assay was performed by diluting an overnight culture 1:50, the culture entered the exponential phase (log phase) faster and a greater dilution of the overnight culture should have been made to clearly distinguish the latent phase. After 5 hours of incubation, the P84 cells are metabolically more active and replicate faster, corresponding to the exponential phase. Finally, after 25 hours, Psa reached the stationary phase and the growth rate start to decrease.

In parallel to the growth curve, a calibration curve was created to enable the quantification of the number of CFUs in a bacterial culture by measuring the OD at 600 nm. The resulting graph is shown in Figure 3.6.
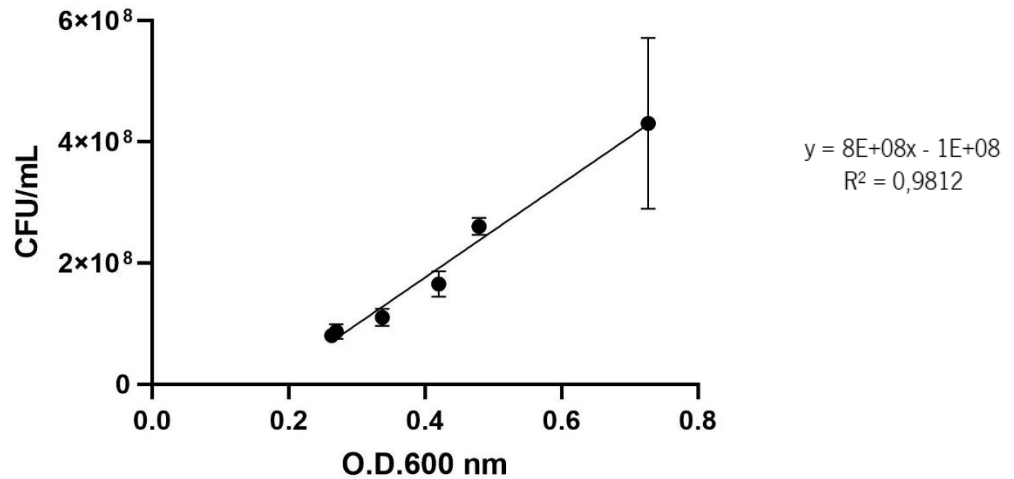
Figure 3.6- Calibration curve of CFU in function of OD (600nm) for P84 Psa strain

3.2. Phage isolation and characterization

3.2.1. Isolation of phages

After the enrichment procedure using the extracts collected from different tissues of the kiwifruit orchards, it was possible to isolate 6 phages targeting Psa host P84 from leaves, stems and trunks from the Guimarães and Póvoa de Lanhoso orchards. Bacteriophages were identified as 8, 10, 18, 66, VC3 and 177T as mentioned in Table 3.2.

Table 3.2- Summary of the phages isolated in this study

	Plant Material	Orchard	Date
8	Leaf	Guimarães	
10	Flower		
18	Leaf	Póvoa de Lanhoso	25/07/2019
33	Leaf	Guimarães	
66			
VC1			
VC2	Branches	Guimarães	19/02/2021
VC3			
VC6			
173T			
175T	Trunk	Guimarães	13/03/2021
177T			

The isolates used in this study were extracted from flowers, leaves, canes and trunk. In addition, extracts obtained from in soil and water samples collected from Psa-infected orchards were also tested for phage isolation, but in the case of this study, there was no growth of phage plaques. The size of the phage plaques tends to be small with an average of 2mm. Phage plaques are quite round, isolated and clear as is possible to see in figure 3.7.
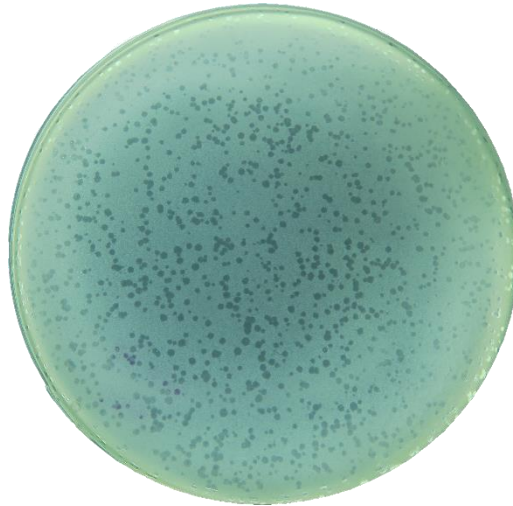
Figure 3.7- Phage 8 isolated on host P84

According to the literature, the phages studied to fight Psa are mostly extracted from soil (Lim *et al.*, 2013; Liu *et al.*, 2021; Park *et al.*, 2018; Yu *et al.*, 2016), water from lagoons and streams (Flores *et al.*, 2020; Ni *et al.*, 2020; Yin *et al.*, 2018), wastewater (Frampton *et al.*, 2014; Martino *et al.*, 2021) and kiwi leaves (Di Lallo *et al.*, 2014).

The phage plaques studied so far have different sizes. Usually all have clear plaques but the size of the plaques can be quite different. In the case of Flores *et al.*, (2020), all selected phages produced large, clear and lytic plaques, but occasionally smaller phage plaques could also be observed. Lim *et al.*, (2013) also describes that the isolated phage under study had large plaques and Martino *et al.*, (2021) phage plaques, clear with 5 mm in diameter. On the contrary, Liu *et al.* (2021) presented that the studied phage would have approximately 2mm in diameter. To prove the variation in size between phage plaques, Di Lallo *et al.*, (2014) demonstrates that one of their phages forms clear plaques with a diameter between 0.5 to 2 mm, and another phage also has clear plaques of larger size, with a diameter of 3 to 7mm. These studies prove the heterogeneity and size diversity among the isolated phages, regardless of their location of extraction.

3.2.2. Host Range

The host range of the isolated phages was evaluated against a collection of 41 Psa strains isolated in this study, as well the reference Psa strains CFBP7286 and P84, *Pseudomonas viridiflava* (strain CFBP2353) and *Pseudomonas syringae* pv. *syringae* (Pss 10604) (Table 3.3)

Table 3.3- Host range of the isolated phages against Psa strain

STRAIN	PHAGES					
	8	10	18	66	VC3	177T
CFBP7286	+	+	+	+	+	+
CFBP2353	-	-	-	-	-	-
Pss 10604	-	-	-	-	-	-
P84	+	+	+	+	+	+
113S	-	-	-	-	-	-
117P	H	-	H	H	+	+
106S	H	H	H	-		-
111F	-	-	-	-	+	+
104S	-	-	-	-	-	-
115F	H	H	H	H	H	-
112F	H	-	H	-	-	-
107F	H	H	H	H	+	+
113F	H	H	H	H	+	+
120F	H	H	H	H	+	+
119F	H	H	H	H	+	+
108F	H	H	H	H	+	+
388S	-	-	-	-	H	-
102F	H	H	H	H	+	+
123S	-	-	-	-	-	-
121F	-	-	-	-	+	+
112B	+	+	+	+	+	+
23	-	-	-	-	H	-
29	-	-	-	-	+	+
6	-	-	-	-	+	+
4	-	-	H	-	+	+
3	H	-	H	-	+	+
1	-	-	-	-	+	+
22	-	-	-	-	+	+
7	-	-	-	-	+	+
28	+	+	+	+	+	+
5	-	-	-	-	+	+
17	-	-	-	-	+	+

Table 3.3- Host range of the isolated phages against Psa strain (continuation)

27	-	-	-	-	+	+
19	+	+	+	+	+	+
110B	-	-	-	-	+	+
VC2	NT	NT	NT	NT	H	-
VC3	NT	NT	NT	NT	H	-
VC4	NT	NT	NT	NT	H	-
VC5	NT	NT	NT	NT	-	-
124F	NT	NT	NT	NT	+	+
117S	NT	NT	NT	NT	+	+
115S	NT	NT	NT	NT	+	+
101S	NT	NT	NT	NT	+	+
388E	NT	NT	NT	NT	+	+
104B	NT	NT	NT	NT	+	+
21	NT	NT	NT	NT	+	+
% INFECTION	47.05	38.23	50.00	38.23	84.44	71.11

+: Lysis; **-:** No Lysis; **H:** Hazy halo **NT:** Not tested

The lytic spectra results presented in Table 3.3 revealed that phages 8, 10, 18, and 66 had a narrow host range, being only able to infect 47.05%, 38.23%, 50% and 38.23% of the strains tested, respectively. Furthermore, the phage plaques formed by these phages were turbid or very turbid on the strains examined. Phages VC3 and 177T were particularly effective against the majority of the Psa strains tested, infecting 84.44% and 71.11%, respectively. Phages were also tested on different strains that also appear on kiwi fruit orchards, which is the case of *Pseudomonas viridiflava* (CFBP2353) and *Pseudomonas syringae* pv. *syringae* (Pss 10604), but no phage plaques were obtained for both strains. These results showed that the isolated phages are specific for Psa strains, a result also reported by Ni *et al.*, (2021). These authors tested the specificity of the PN09, a lytic phage, against 29 Psa strains and 5 distinct strains (*Vibrio parahaemolyticus*, *Salmonella derby*, *Staphylococcus aureus*, *Pseudomonas aeruginosa*, and two *Escherichia coli* strains). The phage was able to cause lysis in all Psa strains, but not in the other five strains mentioned before. However, other authors (Frampton *et al.*, 2014 and Yin *et al.*, 2018 and Yu *et al.*, 2016) described phages that were not only effective against Psa biovar 3 strains but also against other Psa biovars, like *P. syringae* pv. *tabaci*, *P. syringae* pv. *tomato* and *P. syringae* pv. *phaseolicola*. In the host range experiment conducted by Liu *et al.*, (2021), the phage PHB09

exhibited a narrow host range, with a limited capacity to infect Psa and an inability to infect other *Pseudomonas* sp. strains (*P. orzyhabitans*, *P. fluorescens*, *P. putida*, *P. gessardii*, *P. fragi*, *Enterobacter hormaechei*, *E. cloacae* and *E. coli*).

Based on the results obtained from lytic spectra, phages VC3 and 177T were selected for further studies.

3.2.3. Phage Morphological characterization

Transmission Electron Microscopy (TEM) was used to examine phage morphology, and it was observed that phages VC3 and 177T are members of the *Caudovirales* order, belonging to the *Siphoviridae* and *Myoviridae* families, respectively (Figure 3.8), according to the classification system of the International Committee on Taxonomy of Viruses (Adams *et al.*, 2016).
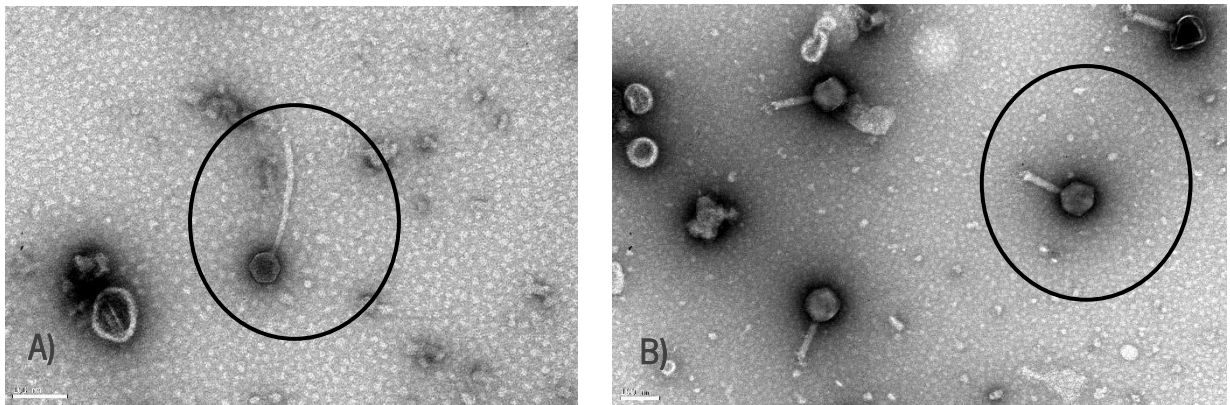
Figure 3.8- TEM visualization of phages' morphology; A) Phage VC3 from *Siphoviridae* family with a non-contractile tail (100 nm scale); B) Phage 177T from *Myoviridae* family with a contractile tail (100 nm scale).

Most of the phages isolated and identified to control Psa belongs to the *Caudovirales* order, the *Myoviridae* family represents for 52.1% of the phages identified and tested to control Psa, while the *Podoviridae* family represents for 41.7% and the *Siphoviridae* family represents for 6.3%(Pereira *et al.*, 2021). *Siphoviridae* phages have lengthy flexible tails, while *Myoviridae* phages have double-layered contractile tails (Yu *et al.*, 2016) .

3.2.4. Phage Stability

The stability of phages to particular environmental conditions like as temperature, pH, and UV radiation is crucial for their practical application as biocontrol agents for plant diseases. As a result, the stability of the two selected phages was measured by counting the number of PFU's following treatment at various temperatures and pH levels, as well as under UV light exposure.

The stability of phages at different temperatures is critical for research with applications that are also affected by environmental factors, as it affects their capacity to adhere, penetrate, and grow within the bacterial host. Only a few phages inject their genome into host cells at temperatures below the optimum, limiting the number of phages participating in amplification. High temperatures cause the latent stage to last longer. Furthermore, high temperatures have the potential to destroy the proteins that make up the capsid (Pereira *et al.*, 2021). In the case of kiwi plants, excessively cold temperatures and frost cause harm to the plants as well as an increase in the spread of Psa as a result of the damage. The stability of the phages at various temperatures was tested and the results are displayed in figure 3.9.
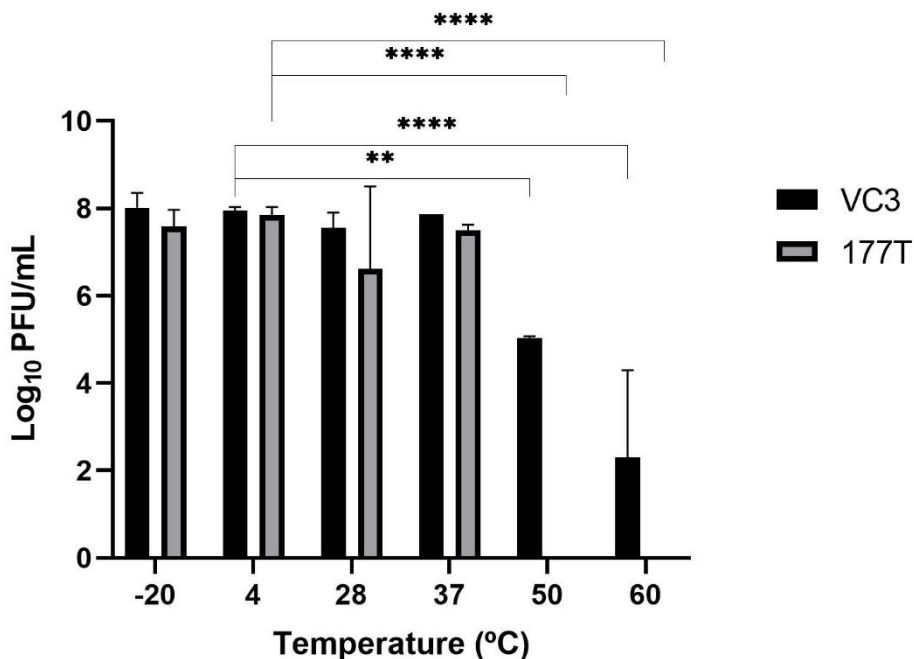
Figure 3.9– VC3 and 177T phage stability at different temperatures (-20°C, 4°C (control) 28°C, 37°C, 50°C and 60°C) during 24 hours. Error bars represent standard deviation for three independent assays performed in duplicate. Statistical analysis was performed by the two-way-ANOVA. ** and **** indicates p≤0.01 and p≤0.0001, respectively.

Phages were tested at various temperatures (-20, 4, 28, 37, 50 and 60°C) to better understand their stability at severe conditions compared to the standard incubation temperature (4°C). As observed in Figure 3.9, phage 177T was stable between -20°C and 37°C and it was completely inactivated in temperatures above 50 °C. Phage VC3 was also stable between -20°C and 37°C with no statistic differences among these conditions. Contrary to phage 177T, after 24h incubation of phage VC3 at 50°C, the majority of the phages remained active although the phage titer dropped 5 $\log_{10}$ PFU/mL comparatively with the control (4°C) (p<0.05), while at 60°C the phage titer decreased 3 $\log_{10}$ PFU/mL (p<0.05).

On studies performed by Di Lallo *et al.*, (2014), Yu *et al.*, (2016) and Park *et al.*, (2018), phages were stable at 40°C after one hour of incubation and phage titer started to decrease when temperatures reached 50°C and phages were inactive at 60°C. Phages isolated by Ni *et al.*, 2021 were stable at temperatures between 25 and 35°C and also decreased when temperatures were above 45 and 55°C, and were also inactive at 60°C. On assays by Flores *et al.*, (2020), phages were tested at the temperatures of 4, 18 and 37°C, and at this last temperature it already shown reduction of titer. Yin *et al.*, (2018) identified phages that were all ineffective between the temperatures of 25 and 60°C. According to Liu *et al.*, (2021), phage PHB09 remained stable for twelve hours at temperatures ranging from 4 to 37°C before starting to lose titer. The phage titer dropped after twenty-four hours at temperatures ranging from 37 to 50°C.

As the average temperature for kiwi fruit growth is 20°C and usually do not reach temperatures above 50°C, the two selected phages are both stable at these cultivation conditions and there's no risk of phage inactivation.

The acidity of the environment is also an important aspect to consider as it influences phage stability, which may ultimately impact phage attachment, infectivity, intracellular replication, and multiplication. Because of their protein nature, phage lifespan reduces slowly as the environment becomes more acidic, inducing irreversible coagulation and precipitation(Pereira *et al.*, 2021). Since phages would be in contact with different environmental conditions when placed in kiwi orchards, it is also critical to address phages' stability to varied pH's, especially because phages can be trapped in biofilms, reversibly adsorbed to soil particles, and inactivated by the soil's low pH (Doffkay *et al.*, 2015). The results obtained are shown in Figure 3.10.
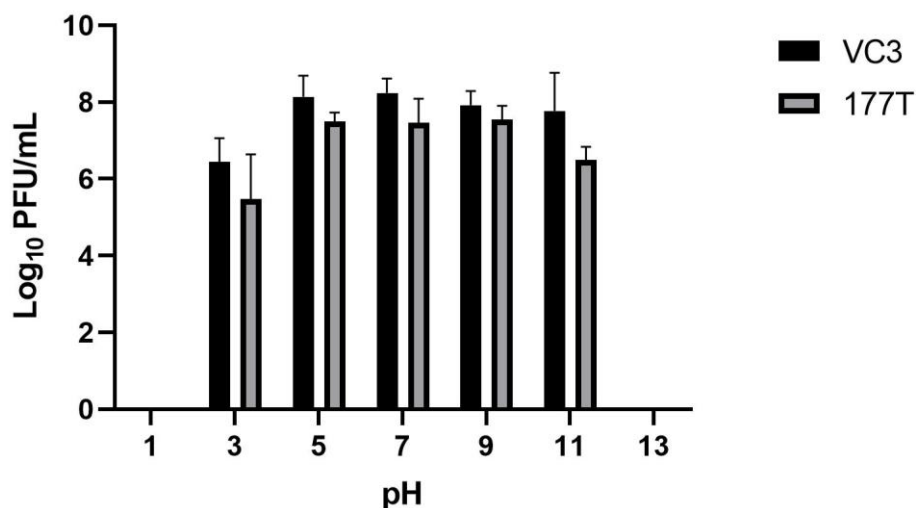
Figure 3.10- VC3 and 177T phage stability at different pH (1, 3, 5, 7(control), 9, 11, 13), for 24h. Error bars represent standard deviation for three independent assays performed in duplicate. Statistical differences were studied with the two-way ANOVA (p<0.05).

The profile of both phages to the different pH's were quite similar. Both phages were particularly sensitive at pH 1 and pH 13 as no phage plaques could be detected after incubation at 4°C for 24 hours at these pH's. In the case of phage 177T, although its concentration decreased on pH 3 and pH 11, no statistic differences were found (p>0.05) comparatively with the control (pH=7). For pH's between pH 5 and pH 9, the concentration of this phage remained stable. On the other hand, the titre of phage VC3 was only lower at pH 3 and was stable between pH 5 and pH 11 with no significant differences were observed (p>0.05).

Other studies regarding the stability of the phage at various pH levels are consistent with the results obtained in this study. For instance, Yu *et al.*, (2016), Park *et al.*, (2018) and Liu *et al.*, (2021) obtained phages with stability between pH 3 and pH 11; however, considerable decreases at pH 3 and pH 11 were seen by Liu *et al.*, (2021). Ni *et al.*, (2021) had great stability between pH 6 and pH 9, decreased at pH 2 and inactivated at pH 1, the phage concentration was relatively high at pH 12. In the study by Yin *et al.*, (2018) the phages were stable between pH2 and pH 12. Flores *et al.*, (2020) only studied stability at pH 4, 5 and 6 where all phages are stable except for one which had little stability at all three pH's. Due to the field conditions not being found pH 1 or 13, in which the phages are shown to be inactive, and therefore, in the pH conditions to which they will be exposed when applied, the phages can be stable.

The phage's ability to survive in the phyllosphere is influenced by UV light. UV light (100–400 nm) is biologically detrimental because it causes protein breakdown in free phage particles and changes the nucleic acid structure, lowering the phage's infectivity (Pereira *et al.*, 2021).The durability of phages against UV rays, in addition to temperature and pH is critical for this study since the major goal is to apply the phages to plants that are exposed to UV rays outside in orchards. As illustrated in Figure 3.11, the stability of these two phages to UV radiation at 366 nm was tested.
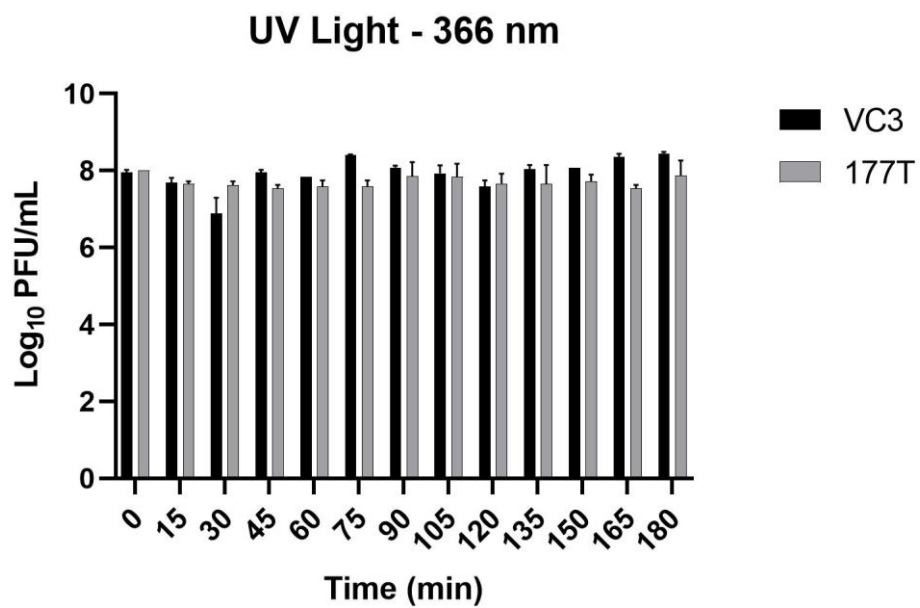
Figure 3.11- VC3 and 177T phage stability at UV light (366nm) at different time points (0 (control), 15, 30, 45, 60, 75, 90, 105, 120, 135, 150, 165 and 180 minutes). Error bars represent standard deviation for two independent assays performed in duplicate. Statistical differences were studied with the two-way ANOVA (p<0.05).

According to the results shown in the figure 3.11, both phages were stable to UV-A rays (366nm) during the 180 minutes of the study and no significant differences were observed (p>0.05). In studies by Yu *et al.*, (2016) and Park *et al.*, (2018), both tested their phages in UV-A (365 nm) and UV-B (306 nm) light and both had similar results. Yu *et al.*, (2016) observed phage stability up to 60 minutes of study at 365 nm wavelengths, while at 306 nm wavelength all phages had a 50% reduction in efficacy. Park *et al.*, (2018) also determined that the PPPL-1 phage was stable in UV-A light but its stability rapidly declined in UV-B light. When tested with UV radiation at 365 nm, Liu *et al.*, (2021) reported that phage PHB09 remained stable for up to 60 minutes.

41

In another approach, Flores *et al.*, (2020) directly tested the phages to solar radiation in 30- and 60-minute trials. The results were maintained in the two periods of study, which determines a good stability of the phages to solar radiation.

3.2.5.   One Step Growth Curve

One-step growth curves are used to determine phage growth parameters such as the latency period and the burst size (Clokie *et al.*, 2018).

Whenever the bacteria is destroyed, it is done by bursting. Phage corpuscles proliferate continuously within the bacterial cell and are always released when the cell ruptures. However, the time required for fixation, the time required for bacterium rupture, and the number of young phage corpuscles developing within the bacterium to be liberated with its rupture all differ in each case, depending on a variety of conditions that differ from one experiment to the next (Hyman & Abedon, 2009). These parameters are represented in Figure 3.12.
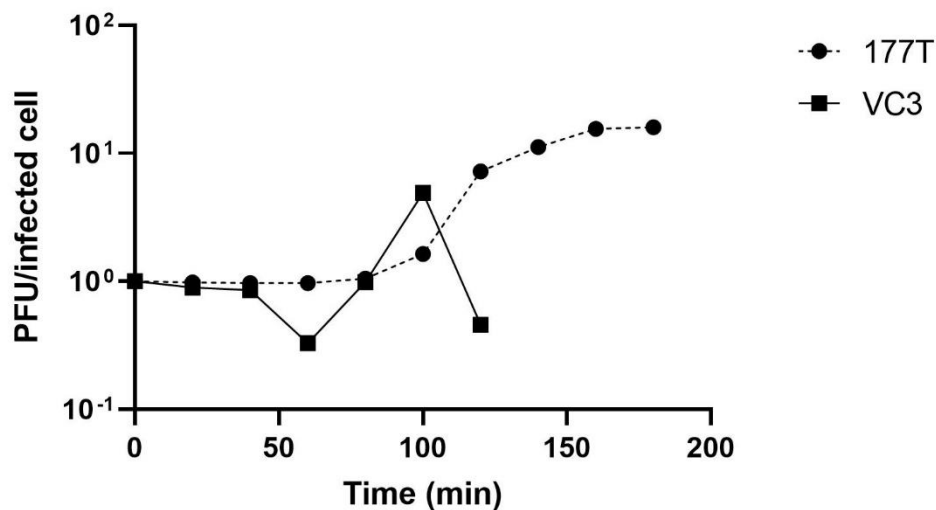
Figure 3.12- One-Step Growth Curve of 177T and VC3 phages

In the diagram above, phage 177T has an 80-minute latency time, a rise period of 60 minutes and a burst size of 14, while phage VC3 it was not possible to obtain a typical OSGC curve and it could be necessary to make some optimizations to the protocol used, such as carrying out

adsorption assays to verify if the 5 minutes of adsorption used are enough for the phages to adsorb to the cells. The latency period is determined by how long the PFU number remains constant and does not show an increase. Latent-period termination occurs for lytic phages during lysis, i.e., when phage offspring are released. Adsorption of phages is the second compound phase, involves a virion collision followed by a virion attachment (Hyman & Abedon, 2009). The sum of these processes determines the phage development time and aids in determining phage population growth rates. The amount of phage offspring generated per infection (phage burst size) also influences phage population growth rates (Hyman & Abedon, 2009).

According to the results shown in Table 3.4, the growth parameters of other reported Psa phages reveal that the latency period, the rise period and the burst size can be quite variable according to the phage type. Latency periods can vary between 15 and 100 minutes, rise period between 15 and 100 minutes, and burst size between 51.3 and 200 PFU/infected cell. Comparing with the studies referred to in the table below, the data obtained on 177T phage is in agreement with the limits of variation of the phage growth periods. Regarding the VC3 phage, further studies will be needed to observe a better growth curve.

Table 3.4 - Summary of OSGC parameters of recent studies of phages to control Psa

Phage	Lantency period (min)	Rise period (min)	Burst Size (PFU/infected cell)	Reference
Φ PSA1	100	50	178	Di Lallo *et al.*, (2014)
Φ PSA2	15	15	92	
Φ XWY0013	20	35	100	
Φ XWY0014	15	35	200	Yin *et al.*, (2018)
Φ XWY0026	30	50	170	
Φ 6	100	40	148	Pinheiro *et al.*, (2020)
PN09	20	100	51.3	Ni *et al.*, (2021)
PHB09	60	40	182	Liu *et al.*, (2021)

3.2.6. Phage DNA extraction, genome sequencing and annotation

Initially, DNA was extracted from three phages: VC3, VC6, and 177T (see figure 3.13). Because phage VC3 and VC6 originated from the same batch of composite material samples, the TEM analysis of their morphology and the same lytic spectra revealed that they are probably the same phage. Therefore, from that moment on, only phages VC3 and 177T were used for the remaining studies.
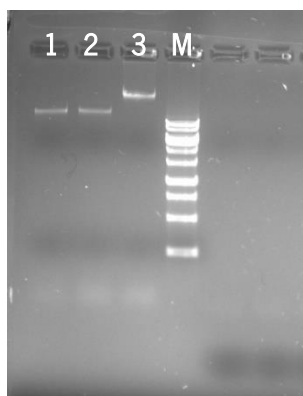
Figure 3.13 – Amplification of VC3, VC6 and 177T DNA, respectively. M: 1kb marker (Grisp).

The values in the table 3.5 represent the quantity of DNA present in each sample in µg/µL, as well as the spectrophotometric absorbance ratio of a sample at 260nm compared to the value obtained at 280nm as a measure of nucleic acid purity and, to a lesser degree, protein purity. The 260/280 ratio is used to assess nucleic acid purity as well as the presence of protein and/or phenol in isolated nucleic acid samples. The 260/230 ratio is useful as a second indicator of purity, indicating the presence of undesirable chemical components.

Table 3.5 – Values obtained at NanoDrop after DNA extraction

Sample	µg/µL	260/280 (nm)	260/230 (nm)
VC3	920.7	1.72	0.37
VC6	1050.8	1.74	0.40
177T	1107.2	1.73	0.42

The NanoDrop equipment's readings indicate that the samples have a high concentration of DNA. Both the 260/280 and 260/230 ratios, on the other hand, have low values. In the instance of the 260/280 ratio, the ideal and pure value would be about 1.8. Although the readings in the

table are over 1.7, they are not close to 1.8, indicating that there is some contamination of acidic phenol or perhaps protein. The 260/230 ratio also has low values, indicating that the sample is likely to include contaminants.

Due to the similarities of samples VC3 and VC6, only one of them, together with phage 177T, were sequenced and compared with other sequenced phages targeting Psa deposited at the National Center for Biotechnology Information (NCBI).

However, it was only phage VC3 was sequenced (outsorcing). The 177T phage could not be sequenced, and one of the possible reasons for this is because, as seen in figure 3.13, the 177T phage band is slightly above the other sample bands. This band might imply that there is bacterial DNA present in addition to phage DNA.

The whole-genome sequencing of phage VC3 revealed that the phage has a double-stranded DNA genome with a length of 50.987 bp and a GC content of 58.7%. After genome annotation, it was possible to find that VC3 phage includes 73 predicted open reading frames (ORFs) ranging between 117 bp and 3675 bp. Based on BLASTP analysis, only 24 genes have with predicted function, while the other 48 encode hypothetical proteins (Figure 3.14). This analysis further revealed 1 tRNA.

The genome of phage VC3 was compared with other phages deposited at NCBI and it was possible to observe a 99.13% on nucleotide identity with PsageK9 phage of (Martino *et al.*, 2021) and 99.82% with ΦPsa1 phage (Di Lallo *et al.*, 2014). The genome organization of the VC3 and PsageK9 phages was highly similar.The presence of an integrase gene and a prophage repressor in both phages characterizes them as lysogenic (Figure 3.15).
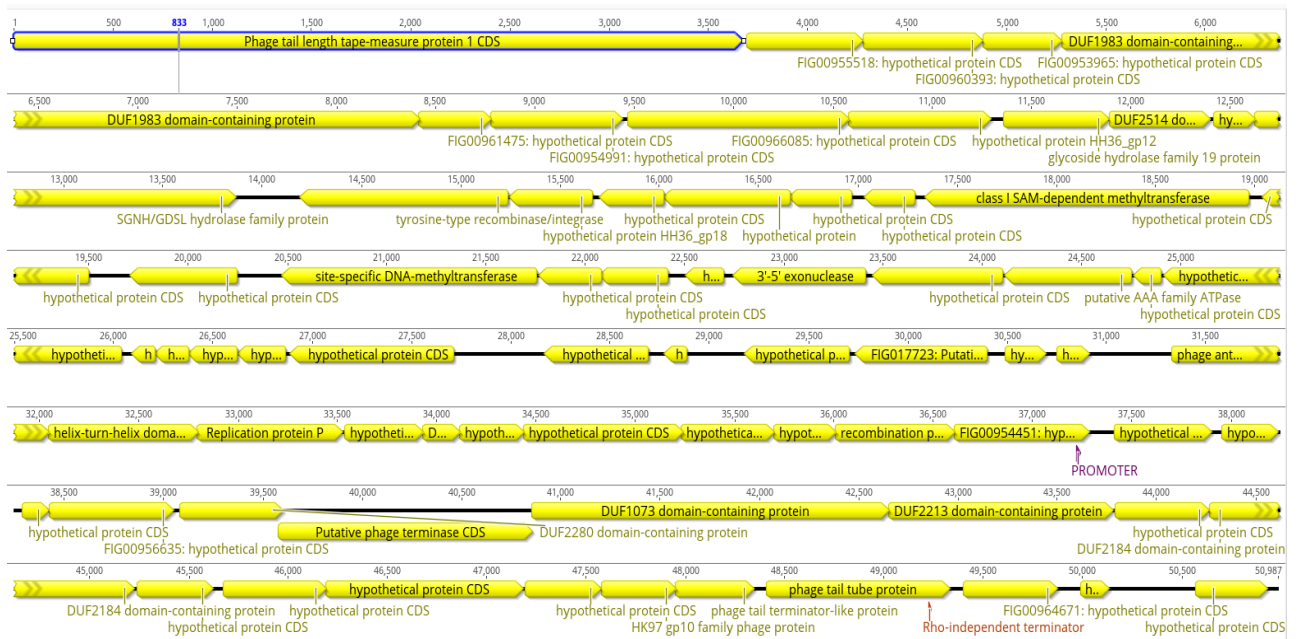
Figure 3.14 – Manual annotation of the VC3 genome on Geneious Prime, where is identified the hypothetical proteins, the proteins with predicted function, a promoter and a Rho-independent terminator (Aragorn server).
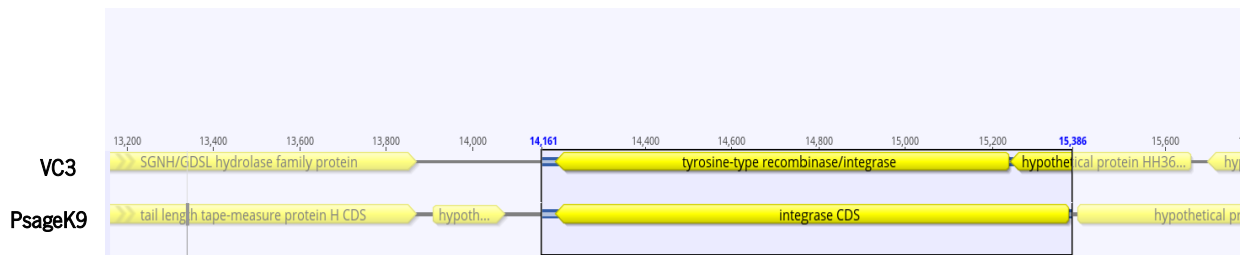
Figure 3.15 – Close up of the presence of integrase CDS on both phages, VC3 and PsageK9, indicating phages to be lysogenic.

Although virulent phages with lytic cycles are the most commonly used for therapeutic or biocontrol purpuses, lysogenic phages, also known as prophages, can aid in the evolution of most bacterial species, including pathogens (Meessen-Pinard *et al.*, 2012). This is the case of prophages that are employed to combat the bacteria like *Clostridium perfringens*, *Pseudomonas aeruginosa, Clostridium difficile, Escherichia coli, Listeria monocytogenes* among others (Monteiro et al., 2019; Swift et al., 2018). Now, breakthroughs in sequencing technology and synthetic biology are opening up new avenues for researchers to investigate the use of temperate phages for bacterial infection treatment. Synthetic biology can now be used to enhance the safety and efficacy of temperate phages in the same way that it can be used to improve the safety and efficacy of strictly lytic phages. Furthermore, temperate phages' distinctive features, such as their ability to integrate into bacterial genomes, can be used in novel therapeutic techniques. Engineering temperate phages to deliver synthetic gene networks that interfere with essential bacterial internal processes in order to cause bacterial cell death is now possible. It's also viable to modify the genome of temperate phages to delete genes essential in lysogenic life cycle maintenance or bacterial pathogenicity. Temperate phages become lytic as a result, and can be employed like any other natural strictly lytic phage, or developed further using synthetic biology techniques (Monteiro et al., 2019).

Most phages isolated to be tested against Psa are lytic, however it is possible to find lysogenic phages in this bacterium (Annex C).

3.1. Infection assays *in vitro*

Features such as adsorption rate and bacterial population lysis contribute to the phage's ability to kill bacteria (Di Lallo *et al.*, 2014). To understand the efficacy of phages against phytopathogenic bacteria, in vitro assays can be performed. In this case, phage infection with both phages 177T and VC3 was performed against a suspended culture of Psa (P84) with an OD_{600} of 0.4 using a MOI =1. After phage infection, and the OD was followed during 48 hours and the results are shown in Figure 3.16.
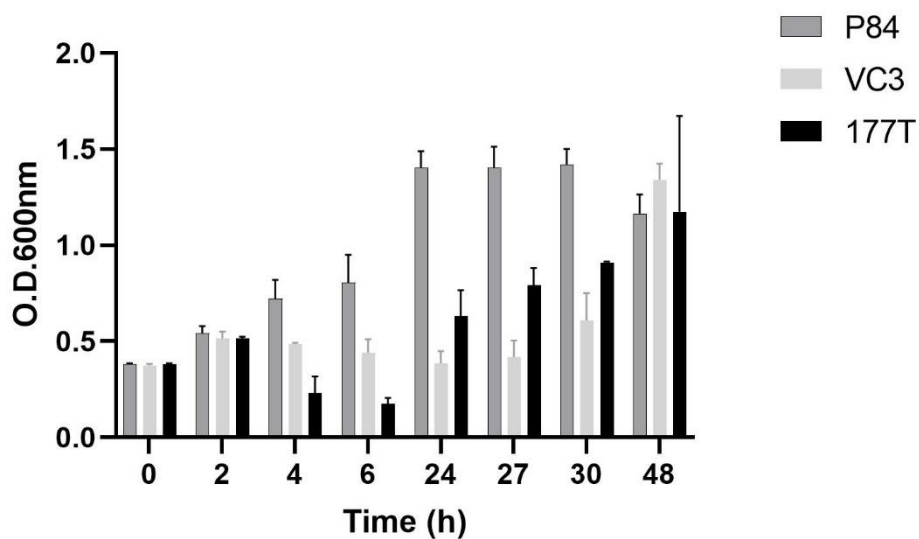
Figure 3.16– Efficacy of phages 177T and VC3 against Psa (strain P84 - Control). Results of *in vitro* experiment. Cell density are shown by OD_{600} at different time points. Error bars represent standard deviation for two independent assays performed in duplicate. Statistical differences were studied with the two-way ANOVA ($p < 0.05$).

When comparing phage 177T and phage VC3 to the control, strain P84, figure 3.13 shows that phage 177T was the first to exhibit a reduction in OD. Four hours after the 177T phage infection, the OD_{600} dropped to 0.172. In the case of phage 177T, he maximum reduction of Psa was achieved 6 hours after phage treatment. A gradual increase of OD_{600} also was visible after 24 hours. In the case of the VC3 phage, it kept the OD low and stable for 24 hours, then steadily declined at 27 hours and climbed after 30 hours of incubation. After 48 hours of incubation, no significant differences were observed when compared with the control ($p > 0.05$).

When comparing results with other studies carried out *in vitro*, Di Lallo *et al.*, (2014) describes the "Time of Death" as the ability of phages to manage to kill the bacteria by their adsorption rate and by the possible reduction in the OD of the bacterial population. In the case of Di Lallo *et al.*, (2014), with an absorbance reading of 600nm at an MOI=0.01 the ΦPSA2 phage determined a kill time of 155 minutes. Because the OD of the bacterial culture never went below its original value, it was impossible to calculate the "time of death" using the ΦPSA1 phage. In this 24-hour investigation, ΦPSA2 significantly reduced bacterial culture turbidity compared to the control, but the turbidity of the ΦPSA1 phage only marginally decreased, with no major changes from the control. In the study developed by Yu *et al.*, (2016), the phages used (MOI=0.01) for in vitro infection had some differences between them. KhuΦ38 demonstrated a late lytic activity compared to KHUΦ59 and KHUΦ74 phages. Lytic activity increased during the first 24 hours after infection but then decreased slightly. KHUΦ34 and KHUΦ44 phages only showed lytic activity after 24 hours of infection. However, the lytic activity of KHUΦ34, KHUΦ38 and KHUΦ 44 phages after 80 hours of treatment was quite similar. The PPPL-1 phage, studied by Park *et al.*, 2018 with MOI=0.01 resulted in a bacterial density gradually reduced to an OD of 0.1 for 12 hours and then slowly increased until the 80h of the study.

Phages tested by Ni *et al.*, (2020) were evaluated with MOI's of 0.1, 1, 10 and 100 and the results showed that phage PN05 inhibited Psa for 12 hours with MOI of 0.1, 1 and 10 and no growth was observed until at 22h of rehearsal where the OD increased from that moment on. With MOI 100, the phage completely inhibited the bacteria up to 24 hours and then some bacterial growth was observed. In the case of PN09 phage, it inhibited bacterial density for 18 hours at an MOI of 0.1, 1 and 10, no bacterial growth was observed until 26 hours of testing and from 26 hours onwards the OD_{600} began to increase slightly, already with MOI =100 the phage inhibited bacterial growth up to 26 hours of assay and soon thereafter had a regrowth after this incubation time. Flores *et al.*, (2020) also tested phages with MOI's of 0.1, 1 and 10 and in all of them, the results showed that the CHF1 phage was the most efficient in causing lysis in the bacterial culture only after two hours of infection, while the CHF19 phage required 6 hours to clear the Psa culture.

Pinheiro *et al.*, (2020) studied the potential application of phage ɸ6, to control Psa in vitro. The study of this phage was tested with two Psa strains, CRA-FRU 12.54 and CRA-FRU 14.10 (two Psa strains biovar 3). The inactivation of Psa was verified in vitro, using liquid culture medium and

in vitro assays, phage ϕ6 was effective against both strains (maximum reduction of 2.2 and 1.9 log CFU/mL for Psa CRA-FRU 12.54 and Psa CRA-FRU 14.10, respectively).

Recently, Liu *et al.*, (2021) tested the phage PHB09 MOI=0.001 and demonstrated that the bacterial density treated with this phage gradually decreased to an OD600 of 0.29 at 12 hours of assay and then slowly increased until 48 hours of incubation.

In general, after analyzing the data of this study and, compared to the data obtained by other authors described above, it is possible to verify that even with different multiplicities of infection (MOI), there is no variation between the phages in terms of performance against the decrease in bacterial growth of Psa. It is also possible to understand that most of the phages mentioned here can obtain a growth inhibition for at least 12 hours, and even with some growth up to 24, 26 or 48 hours, it is possible to see that the phages have good lytic activity to be considered for a biological control of Psa.

3.2. Infection assays *in vivo*

3.2.1. Infection assays *in vivo* in kiwi leaves discs

Given the potential for these phages to be used as biocontrol agents against Psa, it is important to evaluate their performance under laboratory conditions with kiwifruit leaf samples. Leaf discs (2 cm diameter) were used in *in vivo* tests to assess the effect of phages in the Psa load as observed on Figure 3.17.

Phages were individually applied, two hours post Psa infection of the leaf discs. CFUs at various time points were analyzed and no significant differences were observed from the control. Furthermore, phages concentration is decreasing over time and should happen the opposite , the phage could be replicating in the presence of the bacteria and increasing the concentration. The phage could be integrating into the bacteria's genome Phage VC3 showed significant differences between 3h and 48h (p≤0.1). The bacterial density concentration reduced slightly after infection of the VC3 phage, however the greatest outcome was observed 3 hours after application of the phage with a concentration of 7×10^6 CFU/mL, compared to the control with only the Psa strain (1×10^7 CFU/mL). During the rest of the assay VC3 maintained the bacterial load slightly lower than the control ([P84+VC3] $_{T48}$= 4.67×10^6 CFU/mL; [P84] $_{T48}$= 5.67×10^6 CFU/mL). There was no

observation of significant differences between the control and the leaf disks inoculated with P84 and each phage (p<0.05). The method used might possibly be an influence in the results obtained, as homogeneity of the material for phage plaque quantification proved difficult to achieve. In the future, it would be ideal to repeat the test with different extraction techniques as well as MOI 0.1 and 10 to analyze if there are any differences between these results.

Relating the colony quantification data and plaque quantification, it is possible to observe that the data are coherent, where there is an increase in phage plaques (PFU/mL) there is a response of bacterial density reduction (CFU/mL).
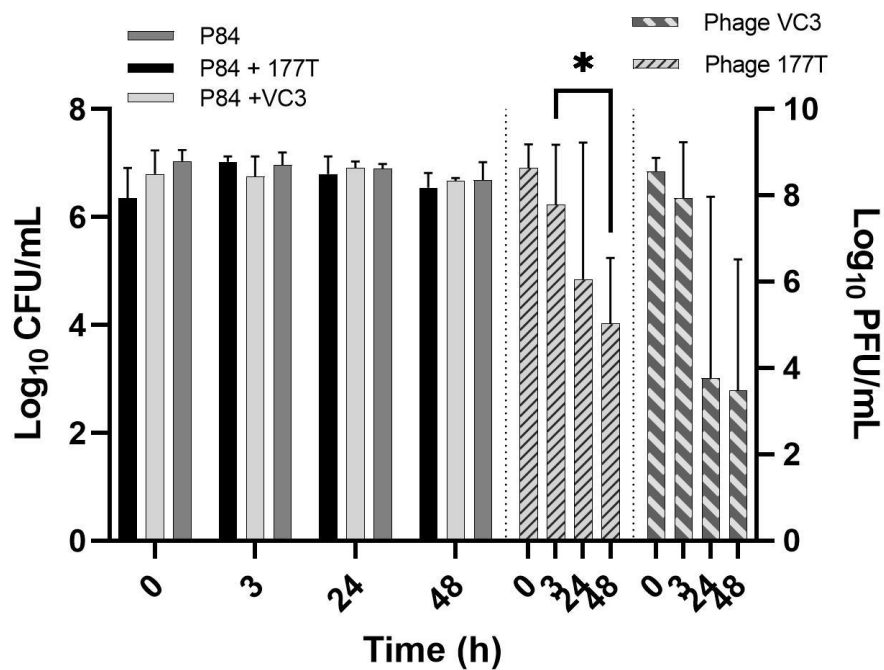
Figure 3.17– Efficacy of 177T and VC3 phages to control Psa in vitro. Bacterial Psa load present in leaf discs inoculated with Psa (dark grey), Psa + VC3 (light grey) and Psa + 177T (black) after 48 hours. Striped bars represent the phage concentration in leaf discs inoculated with the Psa + each phage. Error bars represent standard deviation for two independent assays performed in duplicate. Statistical differences were studied with the two-way ANOVA (p<0.05). * represents significant differences (p≤0.1)

The methodology used in this assay was similar to that one tested by Flores et al., 2020. Their results indicate that a cocktail of their isolated phages CHF1, CHF7, CHF19 and CHF21

managed to reduce the bacterial density of Psa below the limit of detection (20 CFU /mL) after 3 hours of infection, and, Psa remained undetectable up to 24 hours of study. During the same period, the bacterial load of Psa from the leaf discs not treated with phages obtained concentrations between of 10^5 and 10^7 CFU/mL. Bacteriophages were detected throughout the experiment, demonstrating an increase in their concentration at 3 hours, due to Psa replication. The same procedure was used by Liu *et al.*, (2021) in a 72-hour experiment with the PHB09 phage with MOI 1, and it was determined that this phage can lower the bacterial load on kiwi leaves between 24 and 72 hours of infection. Throughout the experiment, phage was detected, with a rise in concentration after 12 hours.

Pinheiro *et al.*, (2020) also developed a similar methodology, using kiwi leaves, cut squares (3cm x 3cm), decontaminated with a 3% H_2O_2 solution (v/v), washed and placed to sterilize in UV light. After sterilization, 100 μL of Psa ($1x10^5$ CFU/mL) and the same volume of phage ($1x10^6$ PFU/mL) were added. Samples were incubated in small petri dishes, placed inside larger petri dishes that contained PBS to prevent dehydration. At each sampling time, the sample was removed and dried, added to PBS and placed in an orbital incubator for 30 minutes. Finally, serial dilutions were made to quantify Psa and phage. The results obtained with this method demonstrated an increase in Psa in the control groups with strains Psa CRA-FRU 12.54 and Psa CRA-FRU 14.10 of 2.2 log and 2.9 log CFU/mL, respectively. Strains CRA-FRU 12.54 and Psa CRA-FRU 14.10 with added phage ϕ 6 obtained a reduction of 0.4 and 0.6 log CFU/mL after 12 hours, respectively, and after 24 hours there was inactivation of 1.1 and 1.8 log CFU/ mL, respectively. Regarding the phage quantification, the phage concentration with strain Psa CRA-FRU 12.54 increased by 1.4 log PFU/mL and with strain Psa CRA-FRU 14.10 it increased to 2.8 log PFU/mL. However, these results are lower that the *in vitro* assay performed by the authors, suggesting that in the ex vivo experiments, the target bacteria may be incorporated inside the leaves' intricate matrix, insulating them from phage particles and preventing phage reproduction.

Through these results obtained by Flores *et al.*, (2020) and by Liu *et al.*, (2021), it is possible to observe that although the use of only one phage is able to reduce the bacterial load of Psa, the use of a phage cocktail may have the best result. The phage cocktail also has the advantage that the phages involved can complement each other and increase the possibility to create a larger host range.

3.3. *Ex vivo* Infection assays in kiwi plants

The preliminary tests in-plant were carried out on a two-year-old, healthy Actinidia *deliciosa* "Hayward". Microlesions were made to aid the bacteria's entrance into the leaf, both on the leaf infected with just Psa and on the leaf treated with a combination of Psa and the phage 177T.

The leaves were observed for a total of 34 days and it was possible to detect that in the leaf infected with only Psa, the differences and the appearance of necrosis by the leaf were notorious. In the case of the leaf inoculated with Psa and phage, the leaf remained without symptoms of Psa (Figure 3.18.).

These preliminary results obtained by visual observation indicate that it is possible to determine that phage 177T will be able to fight Psa infections in the leaves of kiwifruit plants.
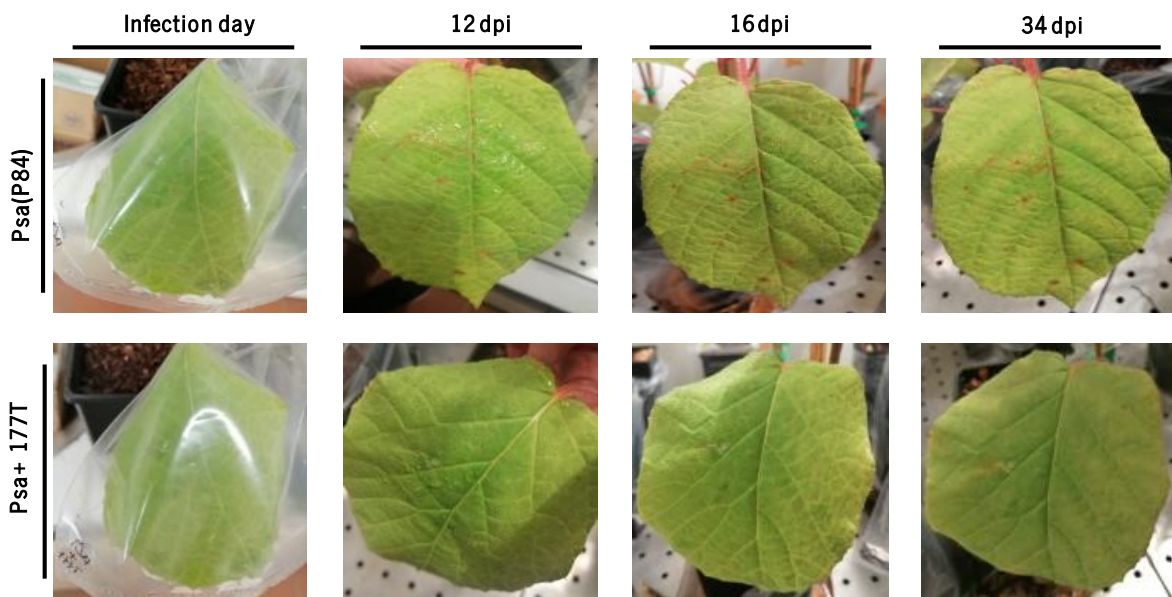
Figure 3.18– Efficacy of 177T phage in a two-year-old *Actinidia deliciosa* "Hayward" plant. Visual pattern Psa symptoms during 12-, 16- and 34-days post infection (dpi). First row, inoculation with Psa, strain P84. Second row, inoculation of Psa and 177T phage.
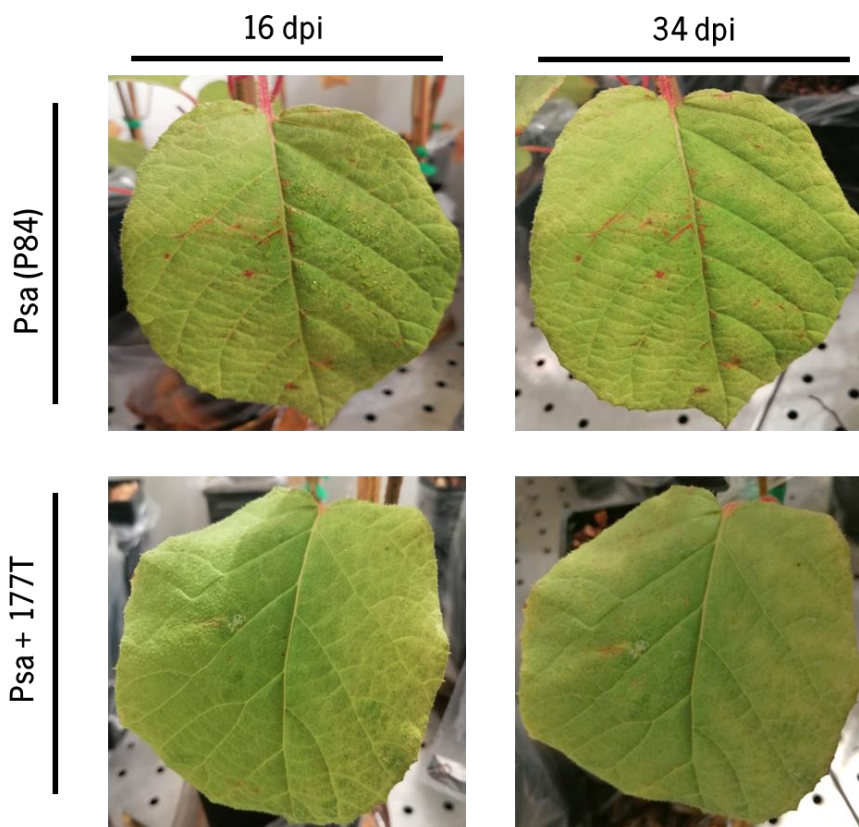
Figure 3.19– Closer look of the differences of leaf infected with Psa (top row) and leaf infected with Psa and 177T phage (bottom row).

To confirm these observations, it would be necessary, in future trials, to quantify the bacteria and phage population, to reach better conclusions. Also in the future, the installation of a larger trial and the spraying of Psa solutions and a combination of Psa and phage may lead to better conclusions and confirm the results obtained in this first trial, which aimed the observation of Psa symptoms.

The results already obtained in in plant trials by other authors who tested combinations of several phages are indicators of the great interest in using phages for biological control of Psa, so it will be necessary to continue with the studies now initiated in this work. Flores *et al.*, (2020), inoculated healthy 2-year plants grown in a greenhouse at 20°C with a regular photoperiod with a bacterial suspension (10^6 CFU/mL) by spraying the suspension directly onto the plant's leaf surface. The quantity of Psa was determined after 24 hours. The author found that the phage cocktail reduced the bacterial load on the leaves by more than 75% when compared to untreated plants that were solely infected with Psa after 24 hours.

In the case of the study by Song *et al.*, (2021) it was used a different method to test phage PPPL-1 on leaves. It was used a silicon brusher to create microlesions and then spread the phage on both sides of the leaf (10^8 pfu/mL). Psa suspension ($OD_{600}=10^8$ CFU/mL) was added after 2 hours. The PPPL-1 control was compared to two additional phages, KHUφ34 and KHUφ38, which were examined separately and in a cocktail of the three phages with a final concentration of 10^8. In comparison to the untreated leaves, the administration of the PPPL-1 phage effectively protected the treated leaves with Psa on the reduction in evident symptomatic spots after 14 days after inoculation. In planta, solo treatment of KHUo34 and KHUo38 phages had less impact than PPPL-1, but a phage cocktail with three phages had equivalent efficacy to PPPL-1 phage alone.

4. Conclusions and future perspectives

The main goal of this study was to isolate, characterize and understand the potential of novel phages against phytopathogenic bacteria present on *Actinidia*, based on preliminary results of this study, it was possible to determine that phages can be a good alternative to antibiotics and also to copper-based products to fight bacterial cancer in kiwi fruit, caused by Psa, and also the disease that causes great economic and productive losses. The phages isolated from composed material of kiwi fruit (VC3) and also from kiwi tree (extract from the trunk – 177T) belong to the *Caudovirales* order, from *Siphoviridae* and *Myoviridae* families, respectively.

The stability testes revealed that the isolated phages can be stable under conditions present in kiwi orchards as they were capable of retaining their efficiency at temperatures ranging from -20°C to 37°C, pH ranging from 3 to 11, and UV radiation resistance.

According to the *in vitro* infection assays performed on suspended cultures, both VC3 and 177T phages were able to reduce the bacterial loads after 4 hours of infection, as measured by the optical density along the time and also observed by a decrease in the quantification of cells and the rise in phage plaques. Although in vivo assays on infected discs did not reveal promsing results as no differences were found between phage infected samples and the control, the preliminary *ex vivo* assays in plants demonstrated visual effects after phage application directly on the leaf.

In the future, significantly more *ex vivo* experiments, large-scale measurement of colonies and phage plaques, and monitoring of symptoms across different parameters would be required. It would also be important to study the combination of multiple phages in a cocktail to understand if the efficacy in biocontrol would increase comparatively with single phage application. Despite the fact that just one phage has been sequenced and confirmed to be lysogenic, prophages might be employed to combat illnesses caused by harmful bacteria. The experiments would be more accurate if the phages were virulent (lytic); consequently, future research should focus on converting these lysogenic phages by genetic modification of genomes, in which the integrase gene, responsible for integration in the host genome, could be removed. Prophages can bestow the capacity to produce poisons, resist antibiotics, boost virulence, and reject subsequent phage infections by modifying the host phenotype, a process known as lysogenic conversion.

5. Bibliographic References

Abelleira, A., Ares, A., Aguín, O., Picoaga, A., López, M. M. & Mansilla, P. (2014). Current situation and characterization of Pseudomonas syringae pv. actinidiae on kiwifruit in Galicia (northwest Spain). *Plant Pathology*, *63*(3), 691–699. https://doi.org/10.1111/ppa.12125

Abelleira, A., Yebra, A., Casal, O. & Vázquez, P. (2015). Método de deteção de Pseudomonas syringae pv. actinidiae (Psa) em ramos assintomáticos de actinídea. *Revista de Ciencias Agrarias*, *38*(2), 206–212. https://doi.org/10.19084/rca.16916

Adams, M. J., Lefkowitz, E. J., King, A. M. Q., Harrach, B., Harrison, R. L., Knowles, N. J., Kropinski, A. M., Krupovic, M., Kuhn, J. H., Mushegian, A. R., Nibert, M., Sabanadzovic, S., Sanfaçon, H., Siddell, S. G., Simmonds, P., Varsani, A., Zerbini, F. M., Gorbalenya, A. E. & Davison, A. J. (2016). Ratification vote on taxonomic proposals to the International Committee on Taxonomy of Viruses (2016). *Archives of Virology*, *161*(10), 2921–2949. https://doi.org/10.1007/s00705-016-2977-6

Azeredo, J., Sillankorva, S. & Pires, D. P. (2014). Pseudomonas Bacteriophage Isolation and Production. In *Methods in molecular biology (Clifton, N.J.)* (Vol. 1149, p. v). https://doi.org/10.1007/978-1-4939-0473-0

Balogh, B., Canteros, B. I., Stall, R. E. & Jones, J. B. (2008). Control of citrus canker and citrus bacterial spot with bacteriophages. *Plant Disease*, *92*(7), 1048–1052. https://doi.org/10.1094/PDIS-92-7-1048

Balogh, B., Jones, J., Iriarte, F. & Momol, M. (2010). Phage Therapy for Plant Disease Control. *Current Pharmaceutical Biotechnology*, *11*(1), 48–57. https://doi.org/10.2174/138920110790725302

Batinovic, S., Wassef, F., Knowler, S. A., Rice, D. T. F., Stanton, C. R., Rose, J., Tucci, J., Nittami, T., Vinh, A., Drummond, G. R., Sobey, C. G., Chan, H. T., Seviour, R. J., Petrovski, S. & Franks, A. E. (2019). Bacteriophages in natural and artificial environments. *Pathogens*, *8*(3), 1–19. https://doi.org/10.3390/pathogens8030100

Bilung, L. M., Pui, C. F., Su'Ut, L. & Apun, K. (2018). Evaluation of BOX-PCR and ERIC-PCR as Molecular Typing Tools for Pathogenic Leptospira. *Disease Markers*, *2018*. https://doi.org/10.1155/2018/1351634

Biolog. (2008). GEN MicroPlate. *Cabot Blvd.*, 1–8.

Borg, T. (2012). COMMISSION IMPLEMENTING DECISION of 5 December 2012 as regards measures to prevent the introduction into and the spread within the Union of Pseudomonas syringae pv. actinidiae Takikawa, Serizawa, Ichikawa, Tsuyumu & Goto. *Official Journal of the European Union*, *335*(2), 49–54.

Boulé, J., Sholberg, P. L., Lehman, S. M., O'Gorman, D. T. & Svircev, A. M. (2011). Isolation and characterization of eight bacteriophages infecting Erwinia amylovora and their potential as biological control agents in British Columbia, Canada. *Canadian Journal of Plant Pathology*, *33*(3), 308–317. https://doi.org/10.1080/07060661.2011.588250

Bryne, D. (2003). Council and Parliament prohibit antibiotics as growth promoters: Commissioner Byrne welcomes adoption of Regulation on feed additives. *Ip/03/1058*, *July*, 2–4.

http://europa.eu/rapid/press-release_IP-03-1058_en.htm?localen%0Ahttp://europa.eu/rapid/press-release_IP-03-1058_en.htm?locale=en

Bukman, P. (1991). Directiva do Conselho de 15 de Julho de 1991 relativa à colocação de produtos fitofarmacêuticos no mercado (91/414/EEC). *Jornal Oficial Das Comunidades Européias*, *230*, 40–52.

Butler, M. I., Stockwell, P. A., Black, M. A., Day, R. C., Lamont, I. L. & Poulter, R. T. M. (2013). Pseudomonas syringae pv. actinidiae from Recent Outbreaks of Kiwifruit Bacterial Canker Belong to Different Clones That Originated in China. *PLoS ONE*, *8*(2). https://doi.org/10.1371/journal.pone.0057464

Buttimer, C., McAuliffe, O., Ross, R. P., Hill, C., O'Mahony, J. & Coffey, A. (2017). Bacteriophages and bacterial plant diseases. *Frontiers in Microbiology*, *8*(JAN), 1–15. https://doi.org/10.3389/fmicb.2017.00034

Cameron, A. & Sarojini, V. (2014). Pseudomonas syringae pv. actinidiae: Chemical control, resistance mechanisms and possible alternatives. *Plant Pathology*, *63*(1), 1–11. https://doi.org/10.1111/ppa.12066

Carvalho, T. P., Nave, A., Rodrigues, S. & Costa, C. A. (2017). Racionalização da luta química no controlo de Pseudomonas syringae pv. actinidea (Psa) na região da Bairrada. *Revista de Ciências Agrárias*, *40*(SP), S103–S110. https://doi.org/10.19084/rca16168

Chan, B. K., Abedon, S. T. & Loc-Carrillo, C. (2013). Phage cocktails and the future of phage therapy. *Future Microbiology*, *8*(6), 769–783. https://doi.org/10.2217/fmb.13.47

Clokie, M. R. J., Millard, A. D., Letarov, A. V. & Heaphy, S. (2011). Phages in nature. *Bacteriophage*, *1*(1), 31–45. https://doi.org/10.4161/bact.1.1.14942

Clokie, M. R., Kropinski, A. M. & Lavigne, R. (2018). Bacteriophages, Methods and Protocols Volume III. In *Methods in Molecular Biology* (Vol. 1681).

Cunty, A., Poliakoff, F., Rivoal, C., Cesbron, S., Fischer-Le Saux, M., Lemaire, C., Jacques, M. A., Manceau, C. & Vanneste, J. L. (2014). Characterization of Pseudomonas syringae pv. actinidiae (Psa) isolated from France and assignment of Psa biovar 4 to a de novo pathovar: Pseudomonas syringae pv. actinidifoliorum pv. nov. *Plant Pathology*, *64*(3), 582–596. https://doi.org/10.1111/ppa.12297

Czajkowski, R., Ozymko, Z. & Lojkowska, E. (2014). Isolation and characterization of novel soilborne lytic bacteriophages infecting Dickeya spp. biovar 3 ('D. solani'). *Plant Pathology*, *63*(4), 758–772. https://doi.org/10.1111/ppa.12157

DGAV. (2013). *Plano de ação nacional para o controlo da flavescência dourada da videira*.

Di Lallo, G., Evangelisti, M., Mancuso, F., Ferrante, P., Marcelletti, S., Tinari, A., Superti, F., Migliore, L., D'Addabbo, P., Frezza, D., Scortichini, M. & Thaller, M. C. (2014). Isolation and partial characterization of bacteriophages infecting Pseudomonas syringae pv. actinidiae, causal agent of kiwifruit bacterial canker. *Journal of Basic Microbiology*, *54*(11), 1210–1221. https://doi.org/10.1002/jobm.201300951

Doffkay, Z., Dömötör, D., Kovács, T. & Rákhely, G. (2015). 59291. *Bacteriophage Therapy against Plant, Animal and Human Pathogens*, *59*(Twort 1915), 291–302.

Donati, I., Buriani, G., Cellini, A., Mauri, S., Costa, G. & Spinelli, F. (2014). New insights on the bacterial canker of kiwifruit (Pseudomonas syringae pv. actinidiae). *Journal of Berry Research*, *4*(2), 53–67. https://doi.org/10.3233/JBR-140073

Donati, I., Cellini, A., Sangiorgio, D., Vanneste, J. L., Scortichini, M., Balestra, G. M. & Spinelli, F. (2020). Pseudomonas syringae pv. actinidiae: Ecology, Infection Dynamics and Disease Epidemiology. *Microbial Ecology*, *80*(1), 81–102. https://doi.org/10.1007/s00248-019-01459-8

Doss, J., Culbertson, K., Hahn, D., Camacho, J. & Barekzi, N. (2017). A review of phage therapy against bacterial pathogens of aquatic and terrestrial organisms. *Viruses*, *9*(3). https://doi.org/10.3390/v9030050

Drzewiecki, J., Latocha, P., Leontowicz, H., Leontowicz, M., Park, Y. S., Najman, K., Weisz, M., Ezra, A. & Gorinstein, S. (2016). Analytical Methods Applied to Characterization of Actinidia arguta, Actinidia deliciosa, and Actinidia eriantha Kiwi Fruit Cultivars. *Food Analytical Methods*, *9*(5), 1353–1366. https://doi.org/10.1007/s12161-015-0309-1

EPA, U. S. (2005). *U.S. EPA, Pesticide Product Label, AGRIPHAGE, 12/09/2005. 3*(c).

EPA, U. S. (2018). *US EPA, Pesticide Product Label, AGRIPHAGE-FIRE BLIGHT,09/27/2018.*

Erwiphage, Zrt, E. & Bendeg, H. (2021). *Nemzeti Élelmiszerlánc - biztonsági Hivatal. 36*(1).

Ferrante, P. & Scortichini, M. (2010). Molecular and phenotypic features of Pseudomonas syringae pv. actinidiae isolated during recent epidemics of bacterial canker on yellow kiwifruit (Actinidia chinensis) in central Italy. *Plant Pathology*, *59*(5), 954–962. https://doi.org/10.1111/j.1365-3059.2010.02304.x

Figueira, D., Garcia, E., Ares, A., Tiago, I., Veríssimo, A. & Costa, J. (2020). Genetic diversity of pseudomonas syringae pv. Actinidiae: Seasonal and spatial population dynamics. *Microorganisms*, *8*(6), 1–18. https://doi.org/10.3390/microorganisms8060931

Flaherty, J. E., Harbaugh, B. K., Jones, J. B., Somodi, G. C. & Jackson, L. E. (2001). H-mutant bacteriophages as a potential biocontrol of bacterial blight of geranium. *HortScience*, *36*(1), 98–100. https://doi.org/10.21273/hortsci.36.1.98

Flaherty, J. E., Jones, J. B., Harbaugh, B. K., Somodi, G. C. & Jackson, L. E. (2000). Control of bacterial spot on tomato in the greenhouse and field with H-mutant bacteriophages. *HortScience*, *35*(5), 882–884. https://doi.org/10.21273/hortsci.35.5.882

Flores, O., Prince, C., Nuñez, M., Vallejos, A., Mardones, C., Yañez, C., Besoain, X. & Bastías, R. (2018). Genetic and phenotypic characterization of indole-producing isolates of Pseudomonas syringae pv. actinidiae obtained from Chilean Kiwifruit Orchards. *Frontiers in Microbiology*, *9*(AUG), 1–12. https://doi.org/10.3389/fmicb.2018.01907

Flores, O., Retamales, J., Núñez, M., León, M., Salinas, P., Besoain, X., Yañez, C. & Bastías, R. (2020). Characterization of bacteriophages against pseudomonas syringae pv. Actinidiae with potential use as natural antimicrobials in kiwifruit plants. *Microorganisms*, *8*(7), 1–17. https://doi.org/10.3390/microorganisms8070974

Frampton, R. A., Pitman, A. R. & Fineran, P. C. (2012). Advances in bacteriophage-mediated control of plant pathogens. *International Journal of Microbiology*, *2012*. https://doi.org/10.1155/2012/326452

Frampton, R. A., Taylor, C., Holguín Moreno, A. V., Visnovsky, S. B., Petty, N. K., Pitman, A. R. & Fineran, P. C. (2014). Identification of bacteriophages for biocontrol of the kiwifruit canker phytopathogen Pseudomonas syringae pv. actinidiae. *Applied and Environmental Microbiology*, *80*(7), 2216–2228. https://doi.org/10.1128/AEM.00062-14

Franco, J. (2008). História e Desenvolvimento Comercial. *Kiwi - Da Produção à Comercialização*, 13–19.

Fujikawa, T. & Sawada, H. (2016). Genome analysis of the kiwifruit canker pathogen Pseudomonas syringae pv. actinidiae biovar 5. *Scientific Reports*, *6*(February), 1–11. https://doi.org/10.1038/srep21399

Gallelli, A., L'Aurora, A. & Loreti, S. (2011). Gene sequence analysis for the molecular detection of Pseudomonas syringae pv. actinidiae: Developing diagnostic protocols. *Journal of Plant Pathology*, *93*(2), 425–435. https://doi.org/10.4454/jpp.v93i2.1198

Garcia, E., Moura, L., Abelleira, A., Aguín, O., Ares, A. & Mansilla, P. (2018). Characterization of Pseudomonas syringae pv. actinidiae biovar 3 on kiwifruit in north-west Portugal. *Journal of Applied Microbiology*, *125*(4), 1147–1161. https://doi.org/10.1111/jam.13943

Gill, J. & Hyman, P. (2010). Phage Choice, Isolation, and Preparation for Phage Therapy. *Current Pharmaceutical Biotechnology*, *11*(1), 2–14. https://doi.org/10.2174/138920110790725311

Guroo, I., Wani, S., Wani, S., Ahmad, M., Mir, S. & Masoodi, F. (2017). A Review of Production and Processing of Kiwifruit. *Journal of Food Processing & Technology*, *8*(10). https://doi.org/10.4172/2157-7110.1000699

He, R., Liu, P., Jia, B., Xue, S., Wang, X., Hu, J., Shoffe, Y. Al, Gallipoli, L., Mazzaglia, A., Balestra, G. M. & Zhu, L. (2019). Genetic Diversity of Pseudomonas syringae pv. Actinidiae Strains from Different Geographic Regions in China. *Phytopathology*, *109*(3), 347–357. https://doi.org/10.1094/PHYTO-06-18-0188-R

Hyman, P. & Abedon, S. T. (2009). Practical methods for determining phage growth parameters. *Methods in Molecular Biology (Clifton, N.J.)*, *501*(June 2014), 175–202. https://doi.org/10.1007/978-1-60327-164-6_18

Jong, H., Reglinski, T., Elmer, P. A. G., Wurms, K., Vanneste, J. L., Guo, L. F. & Alavi, M. (2019). Integrated use of aureobasidium pullulans strain CG163 and acibenzolar-S-methyl for management of bacterial canker in kiwifruit. *Plants*, *8*(8). https://doi.org/10.3390/plants8080287

Lang, J. M., Gent, D. H. & Schwartz, H. F. (2007). Management of xanthomonas leaf blight of onion with bacteriophages and a plant activator. *Plant Disease*, *91*(7), 871–878. https://doi.org/10.1094/PDIS-91-7-0871

Lim, J. A., Jee, S., Lee, D. H., Roh, E., Jung, K., Oh, C. & Heu, S. (2013). Biocontrol of Pectobacterium carotovorum subsp. carotovorum using bacteriophage PP1. *Journal of Microbiology and Biotechnology*, *23*(8), 1147–1153. https://doi.org/10.4014/jmb.1304.04001

Liu, Y., Liu, M., Hu, R., Bai, J., He, X. & Jin, Y. (2021). Isolation of the Novel Phage PHB09 and Its Potential Use against the Plant Pathogen Pseudomonas syringae pv. actinidiae. *Viruses*,

13(2275).

Louws, F. J., Fulbright, D. W., Stephens, C. T. & De Bruijn, F. J. (1994). Specific genomic fingerprints of phytopathogenic Xanthomonas and Pseudomonas pathovars and strains generated with repetitive sequences and PCR. *Applied and Environmental Microbiology*, *60*(7), 2286–2295. https://doi.org/10.1128/aem.60.7.2286-2295.1994

Mallmann, W. . & Hemstreet, C. (1924). Isolation of an Inhibitory Substance From. *Journal of Agricultural Research, ''Washington, D. C*, *XXVIII*(6), 599–602.

Maniloff, J. & Ackermann, H. W. (1998). Taxonomy of bacterial viruses: Establishment of tailed virus genera and the order Caudovirales. *Archives of Virology*, *143*(10), 2051–2063. https://doi.org/10.1007/s007050050442

Mariz-Ponte, N., Regalado, L., Gimranov, E., Tassi, N., Moura, L., Gomes, P., Tavares, F., Santos, C. & Teixeira, C. (2021). A synergic potential of antimicrobial peptides against Pseudomonas syringae pv. actinidiae. *Molecules*, *26*(5). https://doi.org/10.3390/molecules26051461

Martino, G., Holtappels, D., Vallino, M., Chiapello, M., Turina, M., Lavigne, R., Wagemans, J. & Ciuffo, M. (2021). Molecular characterization and taxonomic assignment of three phage isolates from a collection infecting pseudomonas syringae pv. Actinidiae and p. syringae pv. phaseolicola from Northern Italy. *Viruses*, *13*(10). https://doi.org/10.3390/v13102083

Meessen-Pinard, M., Sekulovic, O. & Fortier, L. C. (2012). Evidence of in vivo prophage induction during clostridium difficile infection. *Applied and Environmental Microbiology*, *78*(21), 7662–7670. https://doi.org/10.1128/AEM.02275-12

Melo, L. D. R., Sillankorva, S., Ackermann, H. W., Kropinski, A. M., Azeredo, J. & Cerca, N. (2014). Isolation and characterization of a new Staphylococcus epidermidis broad-spectrum bacteriophage. *Journal of General Virology*, *95*(PART 2), 506–515. https://doi.org/10.1099/vir.0.060590-0

Mohan, S. K. & Schaad, N. W. (1987). An Improved Agar Plating Assay for Detecting Pseudomonas syringae pv. syringae and P. s. pv. phaseolicola in Contaminated Bean Seed. In *Phytopathology* (Vol. 77, Issue 10, p. 1390). https://doi.org/10.1094/phyto-77-1390

Monteiro, R., Pires, D. P., Costa, A. R. & Azeredo, J. (2019). Phage Therapy: Going Temperate? *Trends in Microbiology*, *27*(4), 368–378. https://doi.org/10.1016/j.tim.2018.10.008

Morán, F. (2018). Biodiversity and Biogeography of Three Pseudomonas Syringae Pathovars which Affect Kiwi Fruit Cultivation. *Biodiversity Online Journal*, *1*, 2–4. http://www.fao.org/

Moura, L., Garcia, E., Aguín, O., Ares, A., Abelleira, A. & Mansilla, P. (2015). Identificação e caracterização de Pseudomonas syringae pv. actinidiae (Psa) na Região do Entre Douro e Minho (Portugal). *Revista de Ciências Agrárias*, *38*(2), 196–205.

Ni, P., Wang, L., Deng, B., Jiu, S., Ma, C., Zhang, C., Almeida, A., Wang, D., Xu, W. & Wang, S. (2020). Combined application of bacteriophages and carvacrol in the control of pseudomonas syringae pv. Actinidiae planktonic and biofilm forms. *Microorganisms*, *8*(6). https://doi.org/10.3390/microorganisms8060837

Ni, P., Wang, L., Deng, B., Jiu, S., Ma, C., Zhang, C., Almeida, A., Wang, D., Xu, W. & Wang, S. (2021). Characterization of a lytic bacteriophage against pseudomonas syringae pv. Actinidiae and its endolysin. *Viruses*, *13*(4), 1–16. https://doi.org/10.3390/v13040631

Obradovic, A., Jones, J. B., Momol, M. T., Olson, S. M., Jackson, L. E., Balogh, B., Guven, K. & Iriarte, F. B. (2005). Integration of biological control agents and systemic acquired resistance inducers against bacterial spot on tomato. *Plant Disease*, *89*(7), 712–716. https://doi.org/10.1094/PD-89-0712

OmniLytics Inc. (2018). *Agriphage-Citrus Canker*. 18. https://www3.epa.gov/pesticides/chem_search/ppls/067986-00009-20180927.pdf

OmniLytics Inc. (2019). *Agriphage - Cmm*. *130*(c), 13. https://www3.epa.gov/pesticides/chem_search/ppls/067986-00006-20191202.pdf

Park, J., Lim, J. A., Yu, J. G. & Oh, C. S. (2018). Genomic features and lytic activity of the bacteriophage PPPL-1 effective against pseudomonas syringae pv. Actinidiae, a cause of bacterial canker in kiwifruit. *Journal of Microbiology and Biotechnology*, *28*(9), 1542–1546. https://doi.org/10.4014/jmb.1807.06055

Pereira, C., Costa, P., Pinheiro, L., Balcão, V. M. & Almeida, A. (2021). Kiwifruit bacterial canker: an integrative view focused on biocontrol strategies. *Planta*, *253*(2), 1–20. https://doi.org/10.1007/s00425-020-03549-1

Pinheiro, L. A. M., Pereira, C., Barreal, M. E., Gallego, P. P., Balcão, V. M. & Almeida, A. (2020). Use of phage φ6 to inactivate Pseudomonas syringae pv. actinidiae in kiwifruit plants: in vitro and ex vivo experiments. *Applied Microbiology and Biotechnology*, *104*(3), 1319–1330. https://doi.org/10.1007/s00253-019-10301-7

Pires, D. P., Monteiro, R., Mil-Homens, D., Fialho, A., Lu, T. K. & Azeredo, J. (2021). Designing P. aeruginosa synthetic phages with reduced genomes. *Scientific Reports*, *11*(1), 1–10. https://doi.org/10.1038/s41598-021-81580-2

Pucci, N., Orzali, L., Modesti, V., Lumia, V., Brunetti, A., Pilotti, M. & Loreti, S. (2018). Essential Oils with Inhibitory Capacities on Pseudomonas syringae pv. actinidiae , the Causal Agent of Kiwifruit Bacterial Canker. *Asian Journal of Plant Pathology*, *12*(1), 16–26. https://doi.org/10.3923/ajppaj.2018.16.26

Reglinski, T., Vanneste, J. L., Wurms, K., Gould, E., Spinelli, F. & Rikkerink, E. (2013). Using fundamental knowledge of induced resistance to develop control strategies for bacterial canker of kiwifruit caused by Pseudomonas syringae pv. actinidiae. *Frontiers in Plant Science*, *4*(FEB), 2009–2012. https://doi.org/10.3389/fpls.2013.00024

Robinson, T. P., Ocio, M. J., Kaloti, A. & MacKey, B. M. (1998). The effect of the growth environment on the lag phase of Listeria monocytogenes. *International Journal of Food Microbiology*, *44*(1–2), 83–92. https://doi.org/10.1016/S0168-1605(98)00120-2

Sawada, H., Kondo, K. & Nakaune, R. (2016). Novel biovar (biovar 6) of Pseudomonas syringae pv. actinidiae causing bacterial canker of kiwifruit (Actinidia deliciosa) in Japan. *Japanese Journal of Phytopathology*, *82*(2), 101–115.

Sieiro, C., Areal-hermida, L., Pichardo-gallardo, Á., Almuiña-gonzález, R., de Miguel, T., Sánchez, S., Sánchez-pérez, Á. & Villa, T. G. (2020). A hundred years of bacteriophages: Can phages replace antibiotics in agriculture and aquaculture? *Antibiotics*, *9*(8), 1–30. https://doi.org/10.3390/antibiotics9080493

Sneath, P.H. and Sokal, R.R. (1973). *Numerical Taxonomy: The Principles and Practice of*

Numerical Classification. 1st Edition, W. H. Freeman, San Francisco.

Song, Y. R., Choi, M. S., Choi, G. W., Park, I. K. & Oh, C. S. (2016). Antibacterial activity of cinnamaldehyde and estragole extracted from plant essential oils against Pseudomonas syringae pv. Actinidiae causing bacterial canker disease in kiwifruit. *Plant Pathology Journal*, *32*(4), 363–370. https://doi.org/10.5423/PPJ.NT.01.2016.0006

Song, Y. R., Vu, N. T., Park, J., Hwang, I. S., Jeong, H. J., Cho, Y. S. & Oh, C. S. (2021). Phage pppl-1, a new biological agent to control bacterial canker caused by pseudomonas syringae pv. Actinidiae in kiwifruit. *Antibiotics*, *10*(5), 1–13. https://doi.org/10.3390/antibiotics10050554

Spinelli, F., Donati, I., Vanneste, J. L., Costa, M. & Costa, G. (2011). Real time monitoring of the interactions between pseudomonas syringae pv. actinidiae and actinidia species. *Acta Horticulturae*, *913*(3), 461–466. https://doi.org/10.17660/actahortic.2011.913.61

Stefanowicz, A. (2006). The biolog plates technique as a tool in ecological studies of microbial communities. *Polish Journal of Environmental Studies*, *15*(5), 669–676.

Stewart, a, Hill, R. & Stark, C. (2011). *Desktop evaluation on commercially available microbial-based products for control or suppression of Pseudomonas syringae pv. actinidiae. October*, 26.

Suslow, T. V., Schroth, M. N. & Isaka, M. (1982). Application of a Rapid Method for Gram Differentiation of Plant Pathogenic and Saprophytic Bacteria Without Staining. In *Phytopathology* (Vol. 72, Issue 7, p. 917). https://doi.org/10.1094/phyto-77-917

Swift, S. M., Waters, J. J., Rowley, D. T., Oakley, B. B. & Donovan, D. M. (2018). Characterization of two glycosyl hydrolases, putative prophage endolysins, that target Clostridium perfringens. *FEMS Microbiology Letters*, *365*(16), 1–8. https://doi.org/10.1093/femsle/fny179

Takikawa, Y., Serizawa, S., Ichikawa, T., Tsuyumu, S. & Goto, M. (1989). Pseudomonas syringae pv. actinidiae pv. nov.: The causal bacterium of canker of kiwifruit in Japan. *Japanese Journal of Phytopathology*, *55*(4), 437–444. https://doi.org/10.3186/jjphytopath.55.437

Terms, F. (2011). On an invisible microbe antagonistic to dysentery bacilli . Note by M. F. d'Herelle, presented by M. Roux. Comptes Rendus Academie des Sciences 1917; 165:373–5 . *Bacteriophage*, *1*(1), 3–5. https://doi.org/10.4161/bact.1.1.14941

Tortora, G., Funke, B. & Case, C. (2013). *Microbiology : An Introduction*. Pearson.

Turner, D., Kropinski, A. M. & Adriaenssens, E. M. (2021). A roadmap for genome-based phage taxonomy. *Viruses*, *13*(3), 1–10. https://doi.org/10.3390/v13030506

Twort, F. W. (1915). an Investigation on the Nature of Ultra-Microscopic Viruses. *The Lancet*, *186*(4814), 1241–1243. https://doi.org/10.1016/S0140-6736(01)20383-3

Vanneste, J. L. (2013). Recent progress on detecting, understanding and controlling Pseudomonas syringae pv. Actinidiae: A short review. *New Zealand Plant Protection*, *66*, 170–177. https://doi.org/10.30843/nzpp.2013.66.5594

Vanneste, J. L., Kay, C., Onorato, R., Yu, J., Cornish, D. A., Spinelli, F. & Max, S. (2011). Recent advances in the characterisation and control of pseudomonas syringae pv. actinidiae, the causal agent of bacterial canker on kiwifruit. *Acta Horticulturae*, *913*(February 2009), 443–

456. https://doi.org/10.17660/actahortic.2011.913.59

Vavala, E., Passariello, C., Pepi, F., Colone, M., Garzoli, S., Ragno, R., Pirolli, A., Stringaro, A. & Angiolella, L. (2016). Antibacterial activity of essential oils mixture against PSA. *Natural Product Research*, *30*(4), 412–418. https://doi.org/10.1080/14786419.2015.1022543

Vaz, A., Moura, M. L., Mourão, I. & Pereira, A. M. (2018). Effect of Bacillus subtilis on fruit yield and quality in Actinidia deliciosa orchards infected with bacterial canker in the north of Portugal. *Acta Horticulturae*, *1218*, 253–259. https://doi.org/10.17660/ActaHortic.2018.1218.34

Wicaksono, W. A., Jones, E. E., Casonato, S., Monk, J. & Ridgway, H. J. (2018). Biological control of Pseudomonas syringae pv. actinidiae (Psa), the causal agent of bacterial canker of kiwifruit, using endophytic bacteria recovered from a medicinal plant. *Biological Control*, *116*, 103–112. https://doi.org/10.1016/j.biocontrol.2017.03.003

Woźniak, M., Gałązka, A., Tyśkiewicz, R. & Jaroszuk-ściseł, J. (2019). Endophytic bacteria potentially promote plant growth by synthesizing different metabolites and their phenotypic/physiological profiles in the biolog gen iii microplate™ test. *International Journal of Molecular Sciences*, *20*(21). https://doi.org/10.3390/ijms20215283

Yin, Y., Ni, P., Deng, B., Wang, S., Xu, W. & Wang, D. (2018). Isolation and characterisation of phages against Pseudomonas syringae pv. actinidiae. *Acta Agriculturae Scandinavica Section B: Soil and Plant Science*, *69*(3), 199–208. https://doi.org/10.1080/09064710.2018.1526965

Young, J., Wu, J., Ju Lee, H., Jeong Jo, E., Murugaiyan, S., Chung, E. & Lee, S.-W. (2012). *Biocontrol Potential of a Lytic Bacteriophage PE204 against Bacterial Wilt Tomato*.

Yu, J. G., Lim, J. A., Song, Y. R., Heu, S., Kim, G. H., Koh, Y. J. & Oh, C. S. (2016). Isolation and characterization of bacteriophages against pseudomonas syringae pv. Actinidiae causing bacterial canker disease in kiwifruit. *Journal of Microbiology and Biotechnology*, *26*(2), 385–393. https://doi.org/10.4014/jmb.1509.09012

Zhen, Y., Li, Z. & Huang, H. (2004). Molecular characterization of kiwifruit varieties using SSR markers. *Acta Horticulturae*, *610*(3), 343–349. https://doi.org/10.17660/ActaHortic.2003.610.45

Zheng, X. Y., Spivey, N. W., Zeng, W., Liu, P. P., Fu, Z. Q., Klessig, D. F., He, S. Y. & Dong, X. (2012). Coronatine promotes pseudomonas syringae virulence in plants by activating a signaling cascade that inhibits salicylic acid accumulation. *Cell Host and Microbe*, *11*(6), 587–596. https://doi.org/10.1016/j.chom.2012.04.014

Zehra, A., Naik, H.R., Nayik, G,A., Kour, J., Sangeeta., Bobis, O.,Wani, S.A., Gull, A., Pandita D., Ganaie, T.A. & Nanda,V. (2020). *Antioxidants in Fruits: Properties and Health Benefits.* Springer, Singapore. https://doi.org/10.1007/978-981-15-7285-2_28

6. Annex

Annex A

Table 6.1 – All verified Psa isolates are included in the table below

107F 108F 111F 112F 113F 115F 119F 120F 121F 124F	Leaf	Guimarães	24/05/2019
117P	Petal	Guimarães	24/05/2019
101S 104S 106S 111S 113S 115S 117S 120S 123S 388S	Sepal	Guimarães	24/05/2019
388E	Stamen	Guimarães	24/05/2019
103B 104B 108B 110B 112B	Buds	Guimarães	24/05/2019
1 6 7 17 19 21 22 23 27 28 29	Leaf	Cabeceiras de Basto Braga Póvoa de Lanhoso Cabeceiras de Basto Póvoa de Lanhoso	20/07/2019
3 4	Stem	Cabeceiras de Basto	20/07/2019
5	Stalk	Cabeceiras de Basto	20/07/2019
43 48 50 52 132 135	Leaf	Guimarães	26/06/2020 20/10/2020
6.2. 11.1	Leaf	Famalicão	13/11/2020
V2 V5 VC2	Branches	Guimarães	09/12/2020

Annex B

GEN Ⅲ MicroPlate

A1 Negative Control	A2 Dextrin	A3 D-Maltose	A4 D-Trehalose	A5 D-Cellobiose	A6 Gentiobiose	A7 Sucrose	A8 D-Turanose	A9 Stachyose	A10 Positive Control	A11 pH 6	A12 pH 5
B1 D-Raffinose	B2 α-D-Lactose	B3 D-Melibiose	B4 β-Methyl-D-Glucoside	B5 D-Salicin	B6 N-Acetyl-D-Glucosamine	B7 N-Acetyl-β-D-Mannosamine	B8 N-Acetyl-D-Galactosamine	B9 N-Acetyl Neuraminic Acid	B10 1% NaCl	B11 4% NaCl	B12 8% NaCl
C1 α-D-Glucose	C2 D-Mannose	C3 D-Fructose	C4 D-Galactose	C5 3-Methyl Glucose	C6 D-Fucose	C7 L-Fucose	C8 L-Rhamnose	C9 Inosine	C10 1% Sodium Lactate	C11 Fusidic Acid	C12 D-Serine
D1 D-Sorbitol	D2 D-Mannitol	D3 D-Arabitol	D4 myo-Inositol	D5 Glycerol	D6 D-Glucose-6-PO4	D7 D-Fructose-6-PO4	D8 D-Aspartic Acid	D9 D-Serine	D10 Troleandomycin	D11 Rifamycin SV	D12 Minocycline
E1 Gelatin	E2 Glycyl-L-Proline	E3 L-Alanine	E4 L-Arginine	E5 L-Aspartic Acid	E6 L-Glutamic Acid	E7 L-Histidine	E8 L-Pyroglutamic Acid	E9 L-Serine	E10 Lincomycin	E11 Guanidine HCl	E12 Niaproof 4
F1 Pectin	F2 D-Galacturonic Acid	F3 L-Galactonic Acid Lactone	F4 D-Gluconic Acid	F5 D-Glucuronic Acid	F6 Glucuronamide	F7 Mucic Acid	F8 Quinic Acid	F9 D-Saccharic Acid	F10 Vancomycin	F11 Tetrazolium Violet	F12 Tetrazolium Blue
G1 p-Hydroxy-Phenylacetic Acid	G2 Methyl Pyruvate	G3 D-Lactic Acid Methyl Ester	G4 L-Lactic Acid	G5 Citric Acid	G6 α-Keto-Glutaric Acid	G7 D-Malic Acid	G8 L-Malic Acid	G9 Bromo-Succinic Acid	G10 Nalidixic Acid	G11 Lithium Chloride	G12 Potassium Tellurite
H1 Tween 40	H2 γ-Amino-Butryric Acid	H3 α-Hydroxy-Butyric Acid	H4 β-Hydroxy-D,L-Butyric Acid	H5 α-Keto-Butyric Acid	H6 Acetoacetic Acid	H7 Propionic Acid	H8 Acetic Acid	H9 Formic Acid	H10 Aztreonam	H11 Sodium Butyrate	H12 Sodium Bromate

Figure 6.1 - Biolog Gen III MicroPlate layout

Table 6.2– Summary of sequenced phages targeting Psa

	Host Bacterium	Phage taxonomy		Phage name	Nucleic Acid	Genome size (bp)	Source of Isolation	Country	Year	Accession number	Reference
		Family (morphotype)	Genus								
Lytic phage	Pseudomonas syringae pv. actinidiae	Podoviridae	T7 - like	phiPSA2	linear	40472	sewage	Italy	2014	NC_024362	Di Lallo et al., (2014)
		Podoviridae	T7 - like	phiPsa17	linear	40525	wastewater	New Zeland	2014	NC_047747	Frampton et al., (2014)
		Myoviridae	phiPsa374-like	phiPsa374	linear	98287	soil	New Zeland	2014	NC_023601	Frampton et al., (2014)
		Myoviridae	unclassified	PHB09	circular	94844	soil	China	2021	OK040171	Liu,Y et al., (2021)
		Myoviridae	unclassified	PN05	linear	214121	water	China	2020	MN905546	Ni,P et al., (2020)
		Myoviridae	unclassified	PN09	linear	99229	water	China	2020	MW175491	Ni,P et al., (2020)
		Siphoviridae	unclassified	phiK7B1	linear	112269	unkown	Italy	2020	MT354569	Martino,G et al., (2020)
		unclassified	unclassified	BUCT553	linear	47148	unkown	China	2020	MT941682	Unpublished
		Myoviridae	phiPsa374-like	phiPsa397	linear	98951	unkown	New Zeland	2020	MT670422	Unpublished
		Myoviridae	phiPsa374-like	phiPsa381	linear	98800	unkown	New Zeland	2020	MT670421	Unpublished
		Myoviridae	phiPsa374-like	phiPsa347	linear	99689	unkown	New Zeland	2020	MT670420	Unpublished
		Myoviridae	phiPsa374-like	phiPsa315	linear	98739	unkown	New Zeland	2020	MT670419	Unpublished
		Myoviridae	phiPsa374-like	phiPsa300	linear	99272	unkown	New Zeland	2020	MT670418	Unpublished
		Myoviridae	phiPsa374-like	phiPsa267	linear	100180	unkown	New Zeland	2020	MT670417	Unpublished
		Myoviridae	unclassified	psageK4e	linear	94020	soil	Italy	2021	MZ868713	Martino, G et al., (2021)
		Podoviridae	Rz-like	PPPL-1	linear	41149	soil	South Korea	2015	NC_028661	Park et al.,(2018)
		Myoviridae	unclassified	phiK7A1	linear	98780	soil	Italy	2020	MT740307	Unpublished
		Podoviridae	T7 - like	CHF33	linear	40999	soil	Chile	2020	MN729599	Flores et al., (2020)
		Podoviridae	T7 - like	CHF21	linear	40557	soil	Chile	2020	MN729598	Flores et al., (2020)
		Podoviridae	T7 - like	CHF1	linear	40999	soil	Chile	2020	MN729595	Flores et al., (2020)
		Podoviridae	T7 - like	CHF17	linear	40882	soil	Chile	2020	MN729600	Flores et al., (2020)
		Podoviridae	T7 - like	CHF19	linear	40882	soil	Chile	2020	MN729597	Flores et al., (2020)
		Podoviridae	T7 - like	CHF7	linear	40557	soil	Chile	2020	MN729596	Flores et al., (2020)
Temperate phage	Pseudomonas syringae pv. actinidiae	Siphoviridae	unclassified	phiPSA1	linear	51090	kiwi leaves	Italy	2014	NC_024365	Di Lallo et al., (2014)
		Siphoviridae	unclassified	psageK9	linear	51465	soil	Italy	2021	MZ868718	Martino, G et al., (2021)
		Siphoviridae	unclassified	VC3	linear	50987	compost tree material	Portugal	2021	ND	Rego, R. (2021) - this study